ELSEVIER

Contents lists available at ScienceDirect

# Construction and Building Materials

journal homepage: www.elsevier.com/locate/conbuildmat





# Time-dependent dynamic behavior of rubber-sand mixtures at small to medium strains: Influence of rubber thermal aging and loading history

Kai Zheng <sup>a</sup>, Mengtao Wu <sup>b</sup>, Jun Yang <sup>c</sup>, Wei Liang <sup>a</sup>, Jie He <sup>a</sup>, Fangcheng Liu <sup>a,d,\*</sup>

- <sup>a</sup> College of Civil Engineering, Hunan University of Technology, Zhuzhou, China
- <sup>b</sup> Department of Civil Engineering, Sichuan University, Chengdu, China
- <sup>c</sup> Department of Civil Engineering, The University of Hong Kong, Pokfulam, Hong Kong
- d Intelligent Control of Safety and Risk for Existing Engineering Structures, Key Laboratory of Hunan Province, China

#### ARTICLE INFO

#### Keywords: Rubber-sand mixtures Seismic isolation Time-dependent behavior Loading history Rubber thermal aging

#### ABSTRACT

Rubber-sand mixtures (RSM), characterized by low unit weight, strong elastic deformation ability, good durability, and high energy dissipation, hold significant potential for civil engineering applications. However, research on the time-dependent dynamic behavior remains relatively scarce, limiting their broader application in practical construction. A thorough understanding of this behavior is critical for ensuring long-term performance of RSM across various engineering contexts. In the study, the effects of rubber's thermal aging and loading history, two key factors of time-dependent behavior, on the dynamic properties of RSM under small to medium strains were investigated. Aging of rubber particles was accelerated through oven aging experiments, followed by resonant column tests to determine the dynamic shear modulus and damping ratio of RSM samples with rubber particles of varying aging levels (5 %, 10 %, 15 %, and 20 % rubber content). Furthermore, multiple load tests were also conducted on the same samples to assess the impact of loading history on RSM's dynamic properties. The results reveal that thermal aging causes volumetric expansion and a reduction in compressive strength of rubber particles, leading to changes in the dynamic shear modulus and damping ratio of RSM. Specifically, the dynamic shear modulus initially decreases during early aging stages, then increases, eventually stabilizing, while the damping ratio consistently decreases with prolonged aging. With repeated loading cycles resulting in a reduction in dynamic shear modulus and an increase in damping ratio. These results improve our understanding of this composite's long-term behavior and offer practical advice for its use in seismic isolation and geotechnical engineering.

#### 1. Introduction

As the prevalence of household automobiles increases, the disposal of rubber tires, as a consumable, has become an escalating environmental concern [1,2]. Conventional disposal methods, including incineration and landfilling, are known to cause severe environmental pollution and do not capitalize on the intrinsic properties of rubber. The search for sustainable disposal solutions has been a focal point for researchers. Rubber, characterized by its superior elasticity, lightweight nature, water resistance, and cost-effectiveness, stands out as an ideal material for a range of civil engineering applications [3]. Laboratory and field research has demonstrated that tire-derived rubber crumbs exhibit negligible leaching of substances of particular concern to public health,

substantiating the notion that recycled rubber tires should not be classified as hazardous materials [4–6]. Given its hydrophobic nature, rubber interacts minimally with groundwater, thereby mitigating adverse environmental impacts on soil and groundwater [7]. Consequently, rubber emerges as an eco-friendly engineering material. A plethora of studies have endeavored to integrate rubber into civil engineering [8,9], with rubber-sand mixtures (RSM) being a notable example of such innovation.

Recycling scrap tire rubber through mechanical shredding to produce rubber crumb particles, RSM are created by blending these particles with sand in specific proportions. RSM boasts low cost, straightforward manufacturing processes, and features such as lightweight properties, strong elastic deformation capacity, low shear

<sup>\*</sup> Corresponding author at: College of Civil Engineering, Hunan University of Technology, Zhuzhou, China.

E-mail addresses: kaizhenghut@163.com (K. Zheng), mtwu@scu.edu.cn (M. Wu), junyang@hku.hk (J. Yang), weilianghut@163.com (W. Liang), hejie76@hut.edu.cn (J. He), fcliu@hut.edu.cn (F. Liu).

modulus, and high damping ratio, making it suitable for a variety of engineering applications. For instance, RSM can serve as lightweight fill material for bridge abutments and retaining walls [10–12], for pipe backfilling [13–15], for the treatment of soft soil foundations [16,17], and for road slope construction [1,18,19]. Furthermore, it could be used as a low-cost energy-absorbing material for seismic isolation applications, as corroborated by existing numerical studies [20–27], experimental tests [28–36], and microscopic interpretations [37–39].

It is well-recognized that soils subjected to vibrations induced by earthquakes, traffic loads, wind turbines, etc. cause many geotechnical engineering problems. A thorough understanding of these problems is based on the evaluation of the dynamic response, i.e. shear modulus and damping, before design and construction [40-43]. Therefore, research on the dynamic characteristics of RSM is crucial. Researchers have conducted extensive studies on the dynamic characteristics of RSM [44–47]. In previous research [46], we tested the effect of particle size ratio on the dynamic properties of Resonant Column specimens. Furthermore, we established a new empirical equation to quantitatively analyze the dynamic properties of RSM specimens, in which the predicted values of dynamic shear modulus and modulus damping ratio were in good agreement with the measured values. Madhusudhan et al. [47] conducted a study on the dynamic characteristics of a mix of gap-graded sand and fine rubber tire shreds under undrained, strain-controlled cyclic simple shear (CSS) conditions. The results indicated that the mixture with a 10% rubber content exhibited superior dynamic performance compared to other mixtures. Furthermore, the use of sand-rubber tire shred mixtures helped delay the development of pore pressure. Banzibaganye and Vrettos [45] evaluated the dynamic properties of unsaturated sand-rubber shred mixtures with different weight contents through resonant column tests using fixed-free devices. Finally, design equations for the dynamic response of composite materials were derived based on the experimental results. These studies have reached a consensus: the addition of rubber can decrease the shear modulus of the mixture and increase the damping ratio.

The geotechnical characteristics of soil are subject to temporal variations. During the material's service period, natural deposition, external perturbations, and a multitude of additional factors may impact its properties. It is especially significant to recognize that the mechanical properties of soil undergo gradual changes over time, even under conditions of constant stress. This phenomenon is denoted as Time-Dependent Behavior [48]. While there is a substantial amount of research on Time-Dependent Behavior concerning traditional geotechnical materials [49–52], there is a notable lack of studies focused on RSM. Time-Dependent Behavior is closely linked to the durability of materials, an essential aspect that must be investigated for nearly all construction materials before widespread application. Therefore, it is critical to conduct in-depth research on the influence of Time-Dependent Behavior on the dynamic properties of RSM.

Time-Dependent Behavior primarily encompasses three influencing factors: physical processes, chemical processes, and microbial activity. Research conducted by Anastasiadis et al. [53] has investigated the effects of the duration of consolidation on the dynamic shear modulus and damping ratio of RSM. The results indicated that as the consolidation duration increases, the samples' dynamic shear modulus rises, while the damping ratio decreases. The duration of consolidation is indeed a significant factor influencing Time-Dependent Behavior. As a composite material, the Time-Dependent Behavior of RSM is further influenced by additional factors, including the aging of the material itself and disturbances caused by external forces.

When exploring the Time-Dependent Behavior effects of RSM, we recognize the unique environmental conditions it faces when used as a seismic isolation layer underground. Isolated from light and air, RSM is primarily affected by heat and ground vibrations. In recent years, the uncertainty of the effects of material aging on RSM has hindered its widespread application. Additionally, whether RSM can still maintain good performance after being disturbed by external forces has also been

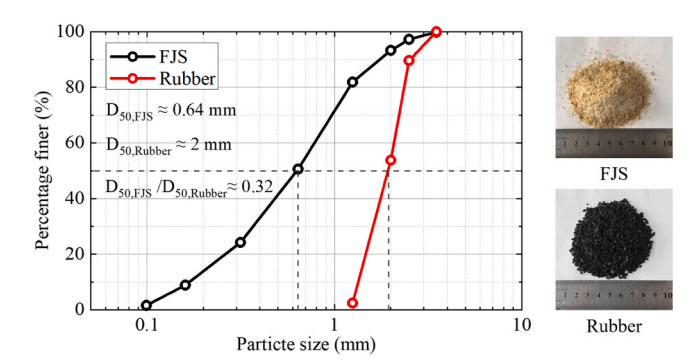


Fig. 1. Grain-size distribution of sand particles and rubber particles (not aged).

a matter of debate. Therefore, we innovatively studied these two factors. First, we subjected rubber particles to aging treatment and tested the compressive performance of rubber particles with different degrees of aging. Then, through a series of resonant column tests, we investigated the influence of the aging degree of rubber particles and loading history on the dynamic shear modulus and damping ratio of RSM under small strain conditions. Furthermore, the analysis delves into the mechanisms underlying the experimental results by examining changes in the fundamental properties of rubber and the interactions between particles. The findings contribute to a better understanding of the influence of Time-Dependent Behavior on the performance of RSM, providing valuable insights for its design in practical applications.

#### 2. Experimental scheme

#### 2.1. Materials

The tested sand was the Fujian sand (FJS) with the  $G_{\rm s,\ FJS}=2.67$ , and the mean particle size  ${\rm D}_{\rm 50,\ FJS}=0.64$  mm. The tested granulated rubber was procured from a local rubber processing factory and was classified as granulated rubber. It consists of scrap tires from which the steel and fibers have been removed. The specific gravity of the rubbers is  $G_{\rm s,\ rubber}=1.1$  and the particle size is  ${\rm D}_{\rm 50,\ rubber}=2$  mm. The main component is natural rubber, primarily composed of polymer isoprene. In addition, the rubber contains other substances, such as vulcanizing agents.

The gradation curves of the sand particles and rubber particles are shown in Fig. 1. To investigate the mechanical effects of thermal aging on the rubber-sand mixture, we subjected the same batch of rubber particles to artificial aging treatment, with specific procedures described in the following text.

## 2.2. Testing equipment

Oven aging experiments effectively replicate the changes in tire material properties associated with natural aging [54]. Therefore, the oven aging method was employed for the accelerated aging treatment of rubber particles. The rubber particles were subjected to accelerated aging treatment using a high-temperature aging test chamber produced by Wuxi Boao Testing Equipment Co., Ltd. This aging chamber allows for the control of temperature, humidity, and duration, enabling precise aging treatment of the materials.

The consolidometer is a commonly used industrial instrument designed to determine the compressive properties of samples under varying loads and confined conditions. It can perform both standard consolidation tests and rapid consolidation tests, measuring the initial consolidation pressure and consolidation coefficient.

The primary testing equipment for this project is the GDS resonant column apparatus, widely regarded as one of the most reliable instruments for measuring the shear modulus of samples at small strains (ranging from  $10^{-6}$  to  $10^{-4}$ ). It has been extensively utilized for advanced testing of sandy soils in various states. Put the soil sample into the

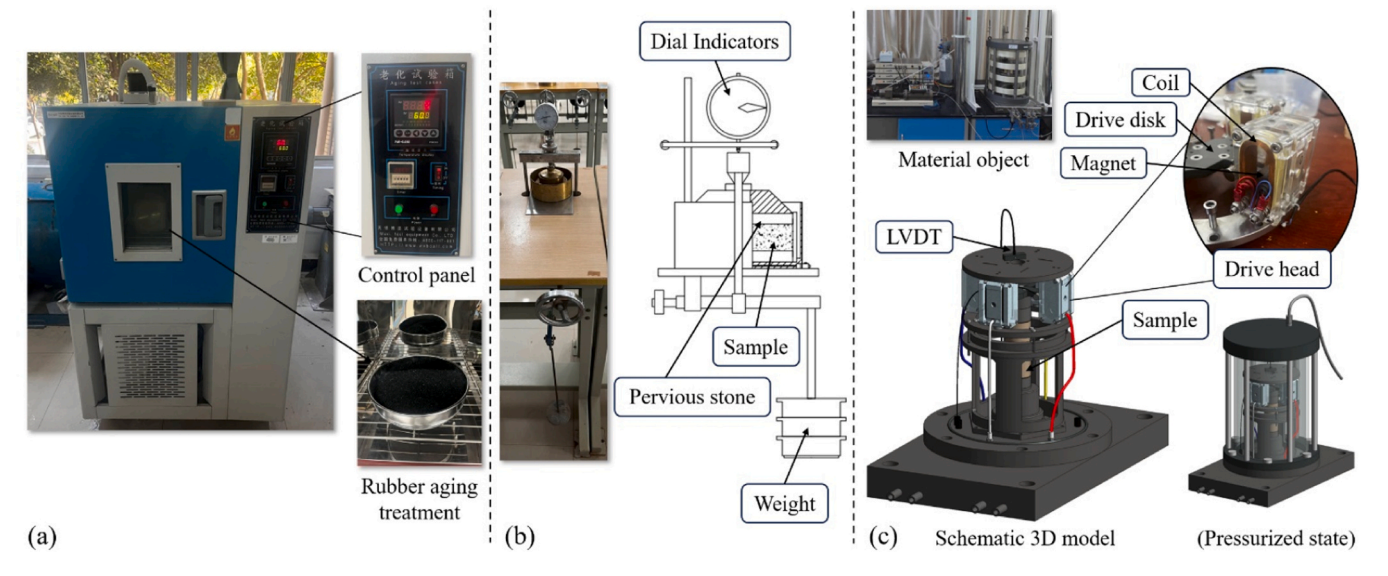


Fig. 2. Experimental equipment. a: High-temperature aging test chamber; b: Consolidometer; c: GDS resonant column system.

resonant column, and apply periodic vibration excitation to the resonant column through the exciter, so that the resonant column resonates. In the resonant state, the vibration frequency of the resonant column is the same as the natural frequency of the soil sample, and the soil sample receives the maximum vibration energy at this time, thereby studying the dynamic characteristics of the soil sample in the resonant state. During the test, the vibration acceleration of the resonant column is measured by the acceleration sensor, and the data is transmitted to the data acquisition system for processing and analysis. By analyzing the vibration acceleration of the resonant column, the shear wave velocity, dynamic elastic modulus, and damping ratio of the soil sample can be obtained.

Descriptive photographs of all equipment are provided in the Fig. 2.

### 2.3. Sample preparation and testing process

## 2.3.1. Accelerated aging treatment of rubber particles using oven method

To simulate the aging effects on rubber particles, an oven method was employed for accelerated aging treatment. The detailed procedure follows: The temperature was set to 60  $^{\circ}$ C, with the humidity between 55 % and 65 %. It was ensured that the oven was properly ventilated, with an external connection to maintain an adequate oxygen supply within the chamber, facilitated by a dedicated air circulation system. Rubber particles from the same batch were placed in the oven for the accelerated aging process. Samples were extracted at intervals of 4, 8,

12, and 16 weeks for subsequent testing. Throughout the aging process, the samples were manually turned daily to ensure uniform thermal aging of the rubber particles. The above methods refer to the research of Rodriguez et al. [55]. The time rubber has spent aging in the oven is used as an indicator of its degree of aging.

#### 2.3.2. Routine consolidation test

The consolidometer is utilized to conduct a confined compression rebound test on rubbers of varying degrees of aging to investigate the impact of aging on the compressive properties of rubber. Initially, the maximum dry density of the unaged rubber  $(\rho_{dmax,\ rubber}=0.72\ g/cm^3)$  is determined through compaction tests, while the minimum dry density  $(\rho_{dmin,\ rubber}=0.42\ g/cm^3)$  is measured using the funnel method. The relative density is set to 0.7, and the controlled density is calculated to be 0.59 g/cm³ using the maximum and minimum dry densities. The mold opening area within the consolidometer is 30 cm², and the sample height is controlled at 2 cm during sample preparation to ensure that the volume of each sample is the same (60 cm³).

Assuming no mass loss during the rubber aging process,  $35.4\,\mathrm{g}$  of rubber of different aging degrees is taken for sample preparation. Each set of samples is subjected to vertical loads of 25 kPa, 50 kPa, 100 kPa, and 200 kPa in sequence, followed by unloading. To ensure that the samples are stable after each loading or unloading, the interval for each reading is greater than 24 hours.

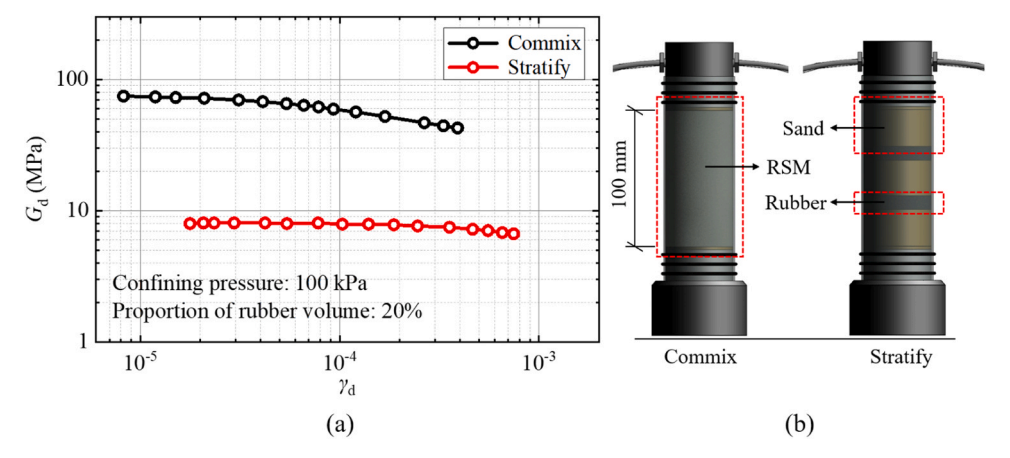


Fig. 3. The impact of the stratification phenomenon on the dynamic properties testing results of RSM.

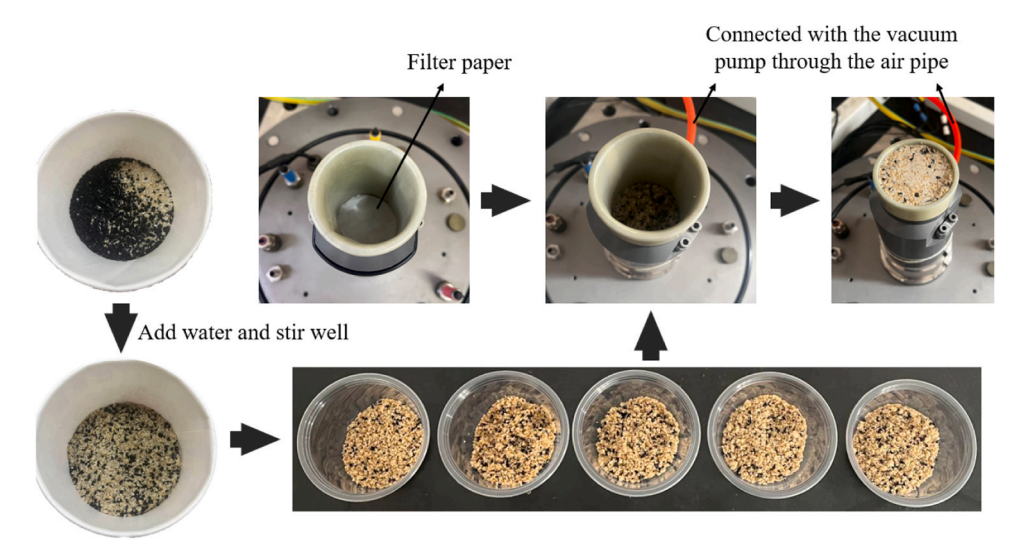


Fig. 4. The schematic diagram of specimen preparation and experimental procedure.

**Table 1**Basic parameters of different materials.

Sample classification	$RC^{\alpha}$	Max. dry density (g/cm <sup>3</sup> )	Min. dry density (g/cm <sup>3</sup> )	Relative Density	Controlling density (g/cm <sup>3</sup> )
Pure sand	-	1.948	1.573	0.7	1.82
Rubber particles	-	0.72	0.417	0.7	0.59
RSM	5 %	1.81	1.34	0.7	1.64
	10 %	1.74	1.22	0.7	1.54
	15 %	1.66	1.17	0.7	1.47
	20 %	1.6	1.03	0.7	1.37

 $\alpha$ : Rubber content ( $RC = m_{\text{rubber}}/m_{\text{RSM}} \times 100$  %, defined as rubber mass as a percentage of RSM mass)

## 2.3.3. Resonant column test

The RSM, prepared by mixing rubber particles with sand in a predetermined ratio, is subjected to a resonant column test. During the specimen preparation, RSM is susceptible to stratification, a phenomenon attributed to the marked disparity in densities between rubber and sand particles, in addition to their distinct particle sizes. Upon the application of external forces, the sand particles tend to descend while the rubber particles ascend, resulting in the formation of layers. As depicted in Fig. 3, the stratified RSM specimens were tested and their performance was juxtaposed with that of the homogenized rubber sand mixtures. It is observed that the stratification significantly influences the experimental data. Furthermore, the stratified samples are prone to developing localized weak spots under the application of confining pressure, which can induce local instability during the resonant column testing phase, thereby adversely impacting the accuracy of the test outcomes.

To mitigate the stratification phenomenon, a multitude of researchers have adopted the approach of consolidating the RSM with the use of consolidating agents; however, this method of treatment can substantially modify the intrinsic properties of the material [56,57]. Empirical trials have revealed that incorporating a measured quantity of water during the specimen preparation phase can significantly enhance the uniformity of RSM. This improvement is attributed to the formation of a thin aqueous film on the particle surfaces, which augments the inter-particle surface tension, thereby promoting greater cohesion among the particles and impeding their inter-granular slippage, as illustrated in Fig. 4. In contrast to alternative consolidants, the incorporation of a modest amount of water is observed to exert a minimal impact on the dynamic mechanical properties of the material. During construction, this preparation method can be used to ensure that the initial state of RSM meets the requirements.

Upon conducting numerous measurements and comparative ana-

lyses, it was determined that at a water content of w=4 % (by mass), the inter-particle mixing within the RSM achieves the highest degree of uniformity, and does not have a great impact on the dynamic characteristics of RSM. At this time, the maximum wet density of RSM reaches the best value. Therefore, 4 % water is incorporated into all specimens, and the maximum wet density  $(\rho_{w \ max})$  is ascertained through compaction testing. The maximum dry density  $(\rho_{d \ max})$  of the specimens is calculated using Eq. (1), while the minimum dry density  $(\rho_{d \ min})$  is directly measured via the funnel method. The relative density is standardized at 0.7, and the controlled density is derived from the maximum and minimum dry densities.

$$\rho_{\rm d max} = \frac{\rho_{\rm w max}}{1 + 0.01w} \tag{1}$$

In practical seismic applications of RSM, e.g., subbuildings as seismic base isolators, the compressibility of the mixture must be controlled because the compressibility of RSM increases [56]. Liu et al. [58] found that the overall rigidity of the RSM is significantly reduced when the rubber volume content (RV) exceeds 50 %. At this time, the mixture embodies the properties of rubber-like particles. When RC=20 %, the rubber volume content is about 50 % ( $RV \approx 50$  %). Therefore, the RC of the sample is controlled within 20 %. In this study, four distinct mass ratios were examined, corresponding to rubber content percentages of 5 %,10 %,15 %, and 20 %. Detailed parameters are delineated in the accompanying Table 1.

The fabrication of the specimen and the experimental workflow are illustrated in Fig. 4, with the detailed operations for sample preparation outlined as follows: i) A vacuum pump is employed to achieve a tight adhesion between the rubber membrane and the mold, with the placement of a filter paper at the base. The soil sample material is evenly partitioned into five segments. Thereafter, one segment of the soil sample is incrementally introduced into the mold. ii) Subsequently, the sample is compacted using a rammer, while concurrently applying

 Table 2

 Sample preparation in torsional resonant column testing program.

Research direction	Specimen	Rubber aging duration (w)	RC	Confining pressure $\sigma_0$ (kPa)	Duration of consolidation (h)
The impact of rubber aging	FJS-R5-T0	0	5 %	50/100/200	>1
	FJS-R10-T0		10 %		
	FJS-R15-T0		15 %		
	FJS-R20-T0		20 %		
	FJS-R5-T4	4	5 %		
	FJS-R10-T4		10 %		
	FJS-R15-T4		15 %		
	FJS-R20-T4		20 %		
	FJS-R5-T8	8	5 %		
	FJS-R10-T8		10 %		
	FJS-R15-T8		15 %		
	FJS-R20-T8		20 %		
	FJS-R5-T12	12	5 %		
	FJS-R10-T12		10 %		
	FJS-R15-T12		15 %		
	FJS-R20-T12		20 %		
	FJS-R5-T16	16	5 %		
	FJS-R10-T16		10 %		
	FJS-R15-T16		15 %		
	FJS-R20-T16		20 %		
The impact of loading history	FJS-R5-D	0	5 %	200	1–60
	FJS-R10-D		10 %		
	FJS-R15-D		15 %		
	FJS-R20-D		20 %		

gentle taps to the mold with a rubber mallet. This compaction routine is reiterated until the sample attains the pre-set height of 20 mm. iii) Before the deposition of the subsequent layer, the surface of the compacted sample is roughened to augment the inter-layer continuity. These procedures are reiterated to finalize the sample assembly, ensuring that each stratum is subjected to an equivalently stringent protocol.

Following the completion of specimen preparation, a pre-established confining pressure is exerted upon the sample, with consolidation being carried out for more than 1 hour after each application of new confining pressure levels. The initiation of testing for the dynamic shear modulus and damping ratio of the sample is contingent upon the stabilization of the soil sample's volume. All procedural steps are conducted in compliance with pertinent standards [59].

In examining the impact of loading history on the dynamic characteristics of RSM, an extended consolidation treatment was applied to each specimen under a confining pressure of 200 kPa. During this procedure, we conducted a series of resonant loadings, with each loading session separated by an interval of approximately 10 hours. The samples configured for the resonant column test are shown in Table 2.

#### 3. Results and discussion

### 3.1. Influence of rubber aging

#### 3.1.1. Rubber particle property variation

After aging treatment, the appearance of rubber particles remains essentially unchanged, with no significant alterations. Sieving of rubber particles with varying degrees of aging and the subsequent replotting of

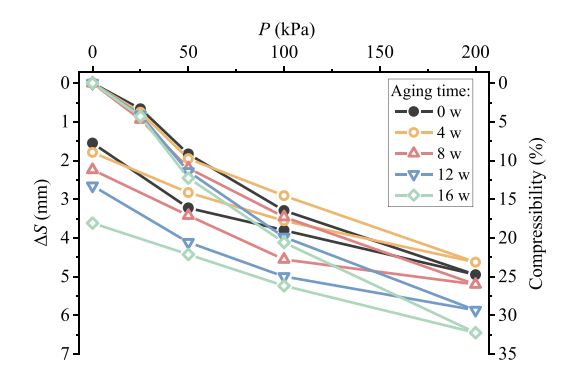


Fig. 6. Effect of aging on the compressive properties of rubber.

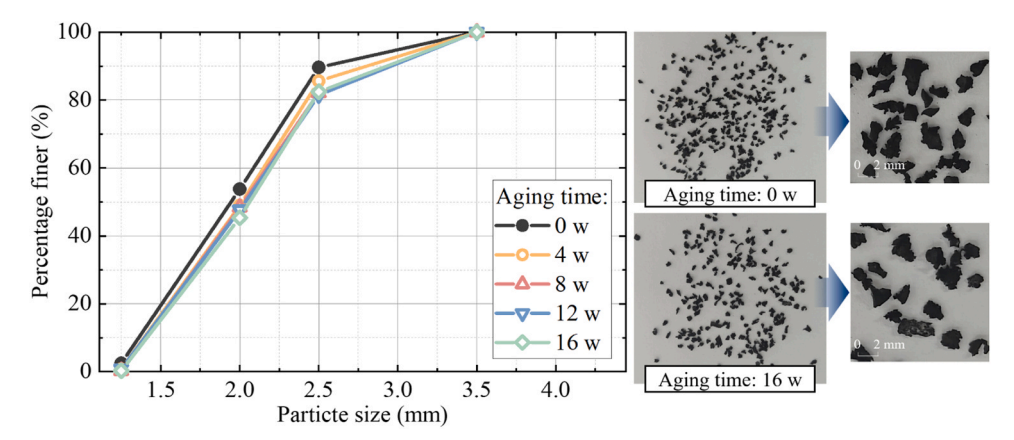


Fig. 5. Gradation curves of rubber particles with varying degrees of aging.

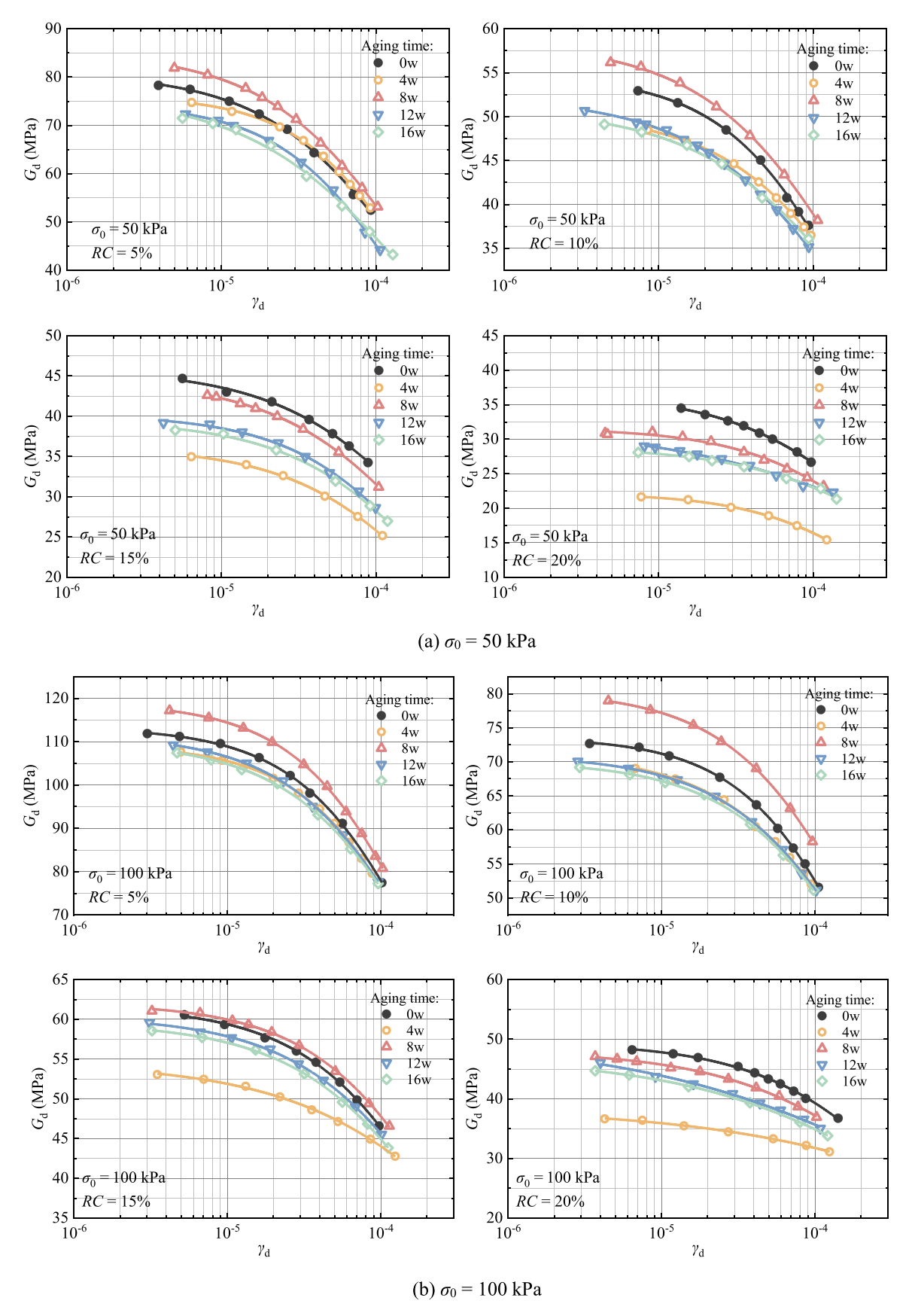


Fig. 7. The influence of rubber aging on the dynamic shear modulus of RSM.

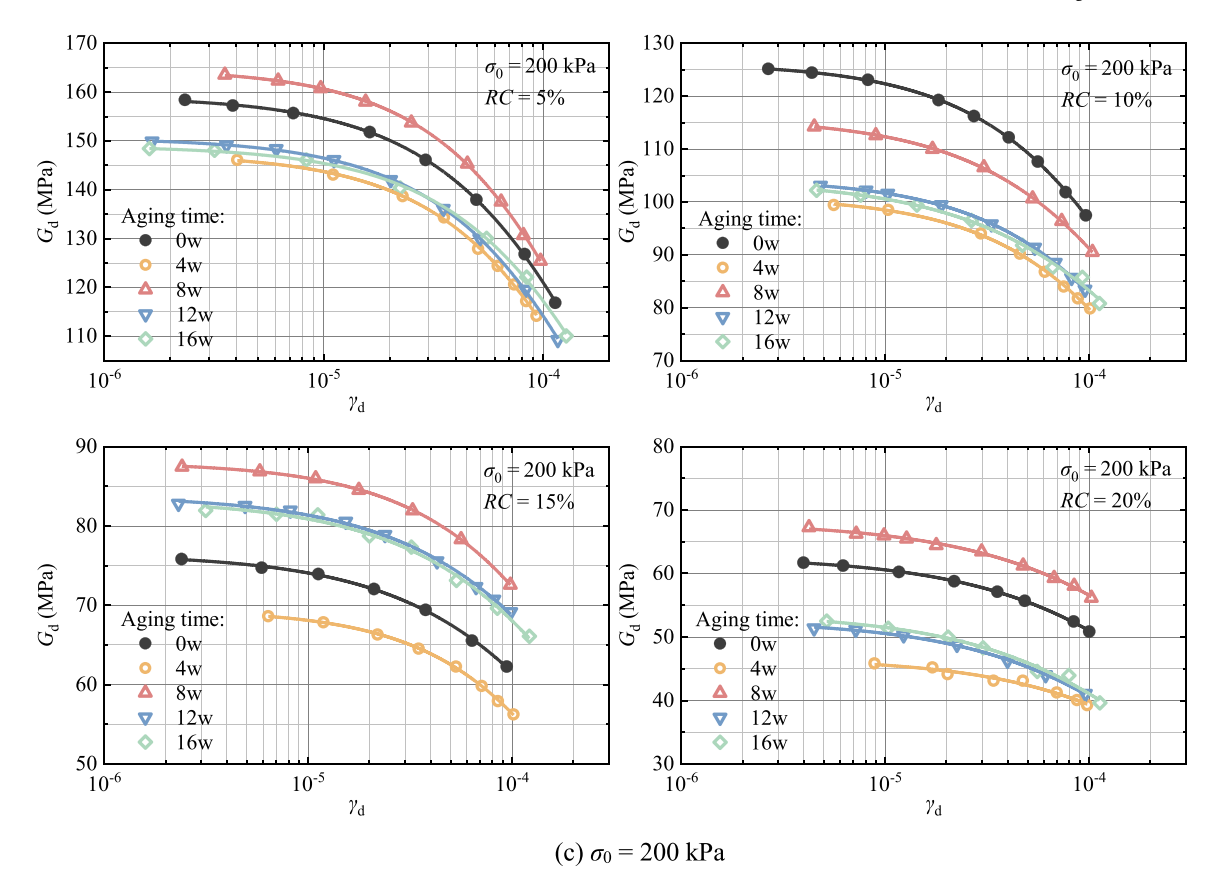


Fig. 7. (continued).

the gradation curves (Fig. 5) demonstrate an increase in particle size with the progression of aging, with the rate of increase tapering off post the fourth week. The phenomenon of volume expansion in rubber particles during the aging process is similar to the findings of Rodriguez et al. [55]. Upon exposure to high-temperature aging treatments, the rubber molecules experience chain scission, a decrease in cross-linking density, and oxidation, which induce structural transformations. These structural modifications lead to a reduction in intermolecular interactions and an enlargement of molecular distances, thereby causing the rubber to exhibit a phenomenon of volumetric expansion. Furthermore, rubber aging can also result in the decomposition or dissolution of additives within the rubber matrix, further contributing to the expansion of the rubber's volume [55]. Severe expansion of foundation materials can indeed lead to engineering problems, such as uneven settlement and structural damage, which are often related to the uplift force of the foundation materials. However, according to the gradation curve data in Fig. 5, the average particle size of rubber particles is approximately 1.9 mm. After aging treatment, the particle size of the rubber particles increases and eventually stabilizes at 2.1 mm, with an average particle size increase of only about 10 % of the original value. This change occurs under conditions of free expansion without external force constraints. When rubber particles are applied to vibration isolation pads, their excellent elasticity further reduces the impact of even minor volume expansion on practical applications. Therefore, we believe that the slight expansion of rubber particles will not have a significant impact on engineering applications.

The compressive characteristics of rubber particles subjected to diverse levels of aging were examined via routine consolidation tests. Fig. 6 illustrates the changes in vertical displacement ( $\Delta S$ ) and corresponding compressibility ( $\Delta S/20~mm \times 100~\%$ ) for different samples during the process of gradually increasing load and subsequent unloading. While rubber is endowed with superior compressive attributes, the process of thermal aging induces molecular chain degradation

within the rubber matrix, consequently affecting its mechanical properties.

Upon comparative analysis of the vertical displacement and compressibility across various samples, it becomes evident that an escalation in aging degree is associated with a progressive reduction in the rubber's compressive modulus. This results in augmented deformation under load, an elevated compression ratio, a diminished capacity for recovery post-unloading, and an increase in permanent deformation. Nonetheless, rubber that has undergone aging treatment for a duration of 4 weeks demonstrated no pronounced alterations in its compressive properties. In fact, under conditions of high load-bearing, an enhancement in the compressive modulus was observed. This observation suggests that the performance characteristics of rubber particles remain largely unaltered before the completion of the 4-week thermal aging process, aligning with the research outcomes reported by Rodriguez et al. [55].

### 3.1.2. Dynamic shear modulus

Resonant column tests were conducted on RSM made of rubber with varying degrees of aging. Fig. 7 illustrates the variation curves of dynamic shear modulus for different samples within the measured strain range. Upon observation of the chart, it can be seen that due to the aging of rubber, the dynamic shear modulus curve of RSM exhibits fluctuations. Overall, the dynamic shear modulus curve of aged RSM is generally lower than that of the unaged samples. This phenomenon indicates that the aging process of rubber leads to a decrease in the dynamic shear modulus of RSM. This reduction in shear modulus is attributed to the significant deformation and rearrangement of the internal particle structure within the specimen when subjected to large strains. Such deformation and rearrangement lead to a decrease in the inter-particle forces, thereby diminishing the specimen's resistance to shear forces, which is reflected in the reduced dynamic shear modulus. Additionally, large strains may induce the destruction or deformation of

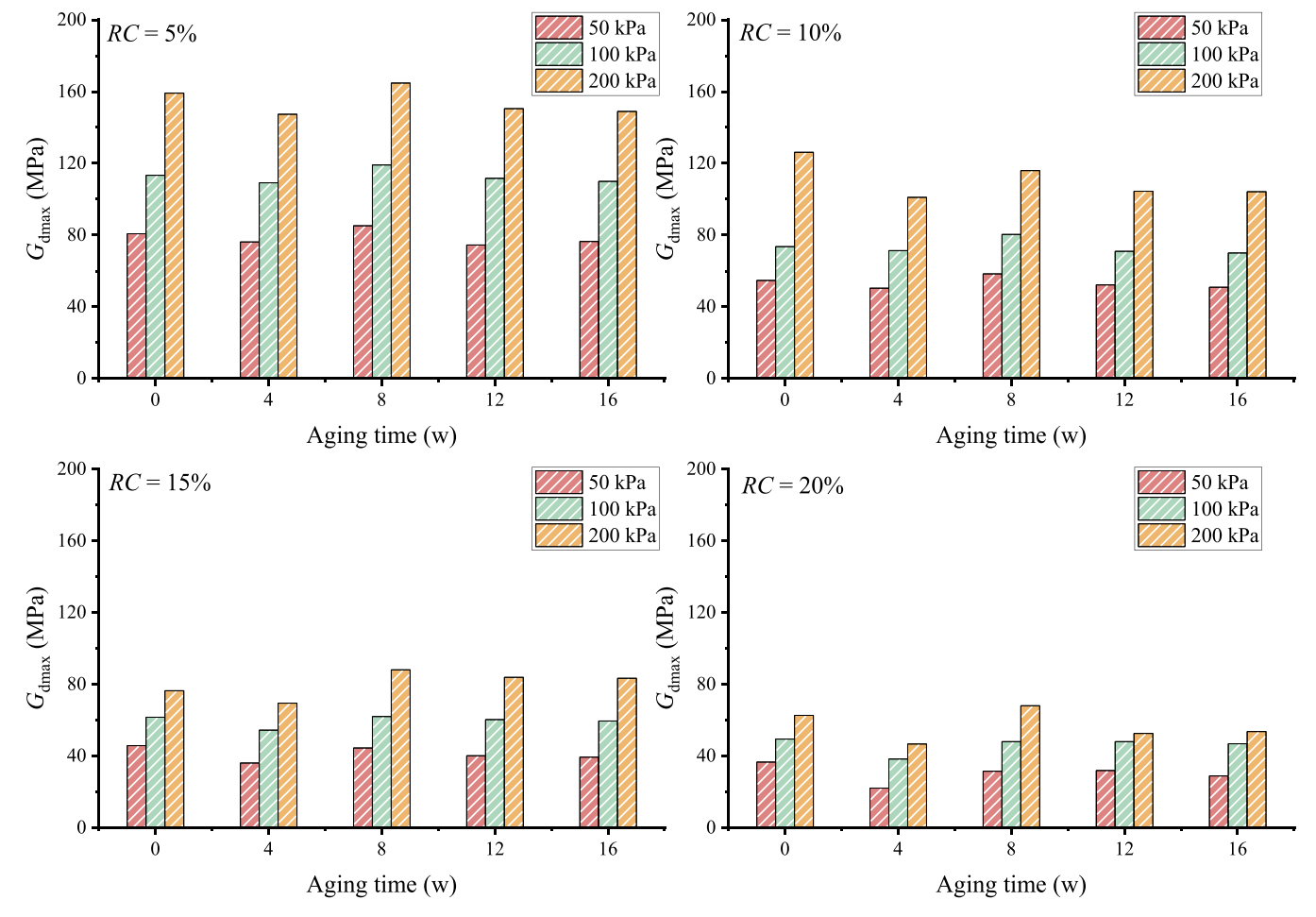


Fig. 8. The influence of rubber aging on the maximum dynamic shear modulus of RSM.

the soil's pore structure, which in turn affects the internal distribution and morphology of the pores. This alteration in the soil's compactness further contributes to the decrease in the dynamic shear modulus of the specimen.

Utilizing this pattern, we can fit the  $G_d \sim \gamma_d$  curve using the classical Hardin and Drnevich equations (Eq. (2)) [60], thereby determining the maximum dynamic shear modulus for each specimen. The maximum dynamic shear modulus serves as a crucial characterization of soil dynamics and a necessary parameter for the dynamic response analysis in geotechnical earthquake engineering.

$$G_{\rm d} = \frac{G_{\rm d max}}{1 + \left(\gamma_{\rm d}/\gamma_{\rm r}\right)^{\alpha}} \tag{2}$$

where  $G_{\rm dmax}$  represents the maximum dynamic shear modulus;  $\gamma_{\rm r}$  denotes the reference shear strain, at which the dynamic shear modulus attenuates to 0.5  $G_{\rm dmax}$ ; and  $\alpha$  is an index parameter greater than 0.

The data points in Fig. 7 were obtained through experimental measurements, while the solid lines in the figure are fits derived from Eq. (2) based on the measured data. Each sample's fitting curve corresponds to a maximum dynamic shear modulus. For ease of observation, the maximum dynamic shear moduli for each sample have been collated and presented in Fig. 8.

The maximum dynamic shear modulus of RSM increases with the rise in confining pressure and decreases with the increase in the RC, which is consistent with the conclusions of many studies. This phenomenon occurs because as the confining pressure increases, the normal stress between particles increases, enhancing the inter-particle friction and consequently increasing the overall compactness of the specimen, leading to an increase in the dynamic shear modulus of the RSM.

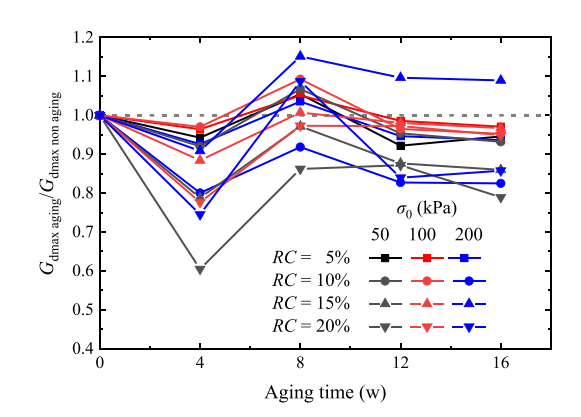
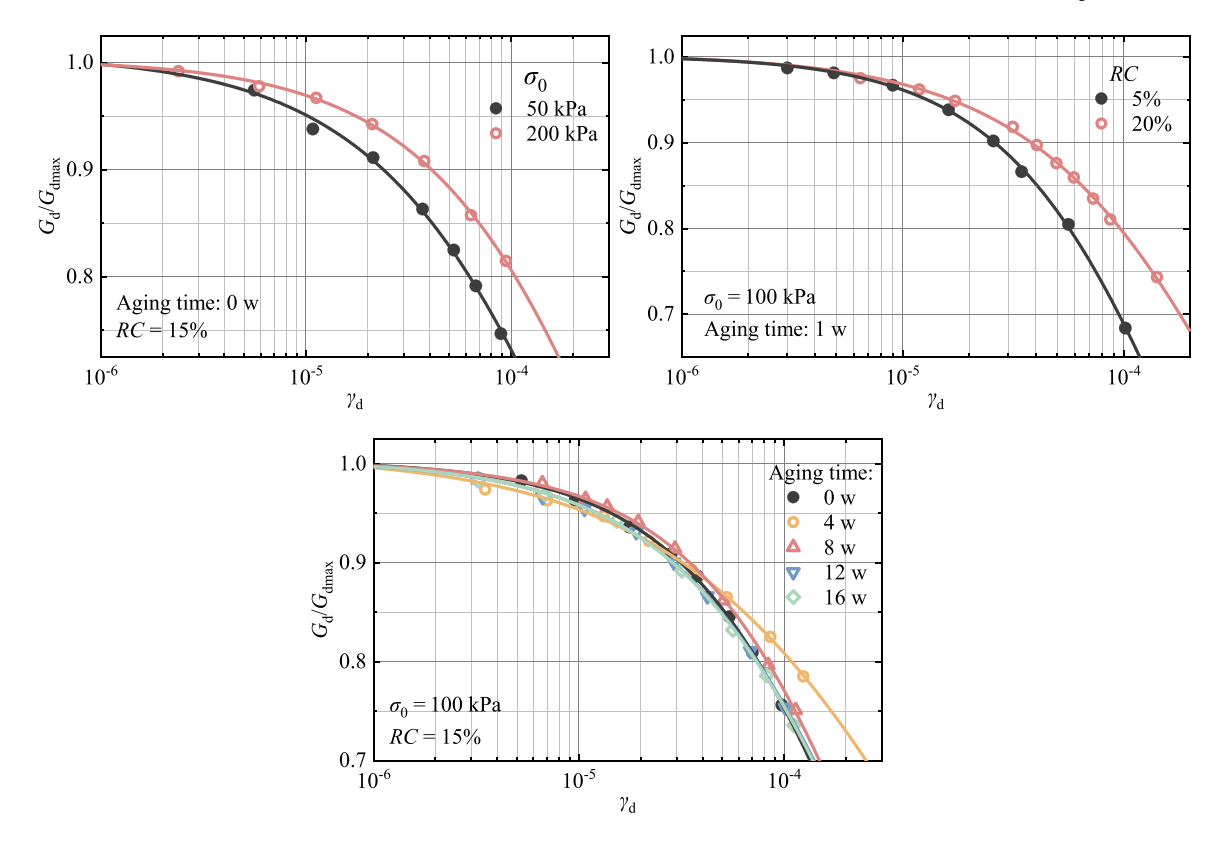


Fig. 9. The trend of the ratio of the  $G_{\mathrm{dmax}}$  of RSM after aging to its initial value.

Rubber, being a soft material, has the effect of reducing the shear modulus of the mixture, and as the *RC* increases, this effect becomes more pronounced.

In Fig. 8, it can be seen that the impact of rubber aging on the dynamic shear modulus of RSM is not monotonic. As the degree of rubber aging increases, the dynamic shear modulus of RSM first decreases, then increases, and finally stabilizes. We believe that the occurrence of this phenomenon may be related to changes in the properties of rubber during the aging process. In the initial four weeks of thermal aging, the volume of rubber expands rapidly. In RSM, while the mass fraction of rubber remains constant, its volume fraction increases, altering the types of particle contacts, with an increase in rubber-rubber and rubber-sand



**Fig. 10.**  $G_d/G_{dmax} \sim \gamma_d$  curves under different influence factors.

contacts. Coupled with the fact that the compressive properties of rubber do not change significantly at this stage, this leads to a reduction in the dynamic shear modulus of RSM. As the aging of rubber progresses, its compressive properties begin to change noticeably. The decrease in compressive performance reduces the rubber's effect on lowering the shear modulus of the mixture, causing an increase in the shear modulus of RSM. Subsequently, as the rate of change in rubber properties slows down and the volume expansion ceases, the dynamic shear modulus of RSM tends to stabilize.

By synthesizing the data from Figs. 7 and 8, we can observe that although the increase in the degree of rubber aging leads to fluctuations in the dynamic shear modulus of RSM, overall, the dynamic shear modulus of the samples treated with aging shows a downward trend. Furthermore, the maximum dynamic shear modulus of RSM, after a period of fluctuation, will stabilize at a value lower than that of the unaged samples, with a relatively small variation. To clearly illustrate the effect of rubber aging on RSM, Fig. 9 presents the variation trend of the maximum dynamic shear modulus of RSM after aging relative to its initial value.

We compared the normalized  $G_{\rm d}/G_{\rm dmax} \sim \gamma_{\rm d}$  curves of confining pressure, RC, and the degree of aging of rubber to analyze the influence of various factors on the degradation curves, as depicted in Fig. 10. The shear modulus of the mixture will decay with the increase of its strain. The gentler the normalization curve in the figure, the slower the decay rate of the material, the weaker the nonlinearity, and the better the elasticity.

In Fig. 10, it can be seen that with the increase of confining pressure or RC, the shear modulus attenuation of RSM slows down, and the elasticity of the material increases. The degree of rubber aging has a negligible effect on the rate of decay of the dynamic shear modulus of RSM. The attenuation curve of RSM fabricated with rubber aged for 4 weeks is relatively flat, suggesting that the RSM possesses the greatest elasticity at this aging period.

## 3.1.3. Damping ratio

Damping ratio is a crucial parameter in soil dynamics, indicating the capacity of soil materials to dissipate energy when subjected to dynamic loading. To effectively serve the purpose of seismic resistance and vibration mitigation, the RSM utilized as isolation layers typically require a higher damping ratio. To investigate the influence of rubber aging on the damping ratio of RSM, we measured the  $D \sim \gamma_d$  curves for each specimen. In Fig. 11, it can be observed that the damping ratio of the specimens decreases with the increase in confining pressure and increases with the increase in RC, which is a generally established conclusion. Additionally, the changes in the damping ratio of RSM caused by rubber aging are not significant. The curves corresponding to the specimens treated with aging are generally positioned below those of the control specimens, indicating that the aging of rubber has somewhat reduced the damping ratio of RSM to a certain extent. This means that with the aging of rubber, the energy dissipation capacity of RSM for vibration isolation decreases, but the extent of the decrease is relatively small.

To further analyze the variation law of the RSM damping ratio, we use the Stokoe and Darendeli dynamic characteristic equation [61] to fit the experimental results of the damping ratio of the mixture.

$$D = b \left(\frac{G_{\rm d}}{G_{\rm d max}}\right)^{0.1} D_{\rm ma sin g} + D_{\rm min} \tag{3}$$

$$D_{\text{ma sin g}} = c1D_{\text{ma sin g},\alpha=1.0} + c2D_{\text{ma sin g},\alpha=1.0}^{2} + c3D_{\text{ma sin g},\alpha=1.0}^{2}$$
 (4)

$$D_{\text{ma sin g},\alpha=1.0}\left(\%\right) = \frac{100}{\pi} \left[ 4 \frac{\gamma_{\text{d}} - \gamma_{\text{r}} \ln\left(\frac{\gamma_{\text{d}} + \gamma_{\text{r}}}{\gamma_{\text{r}}}\right)}{\frac{\gamma_{\text{d}}^2}{\gamma_{\text{d}} + \gamma_{\text{r}}}} \right]$$
(5)

$$c1 = -1.1143\alpha^2 + 1.8618\alpha + 0.2523 \tag{6}$$

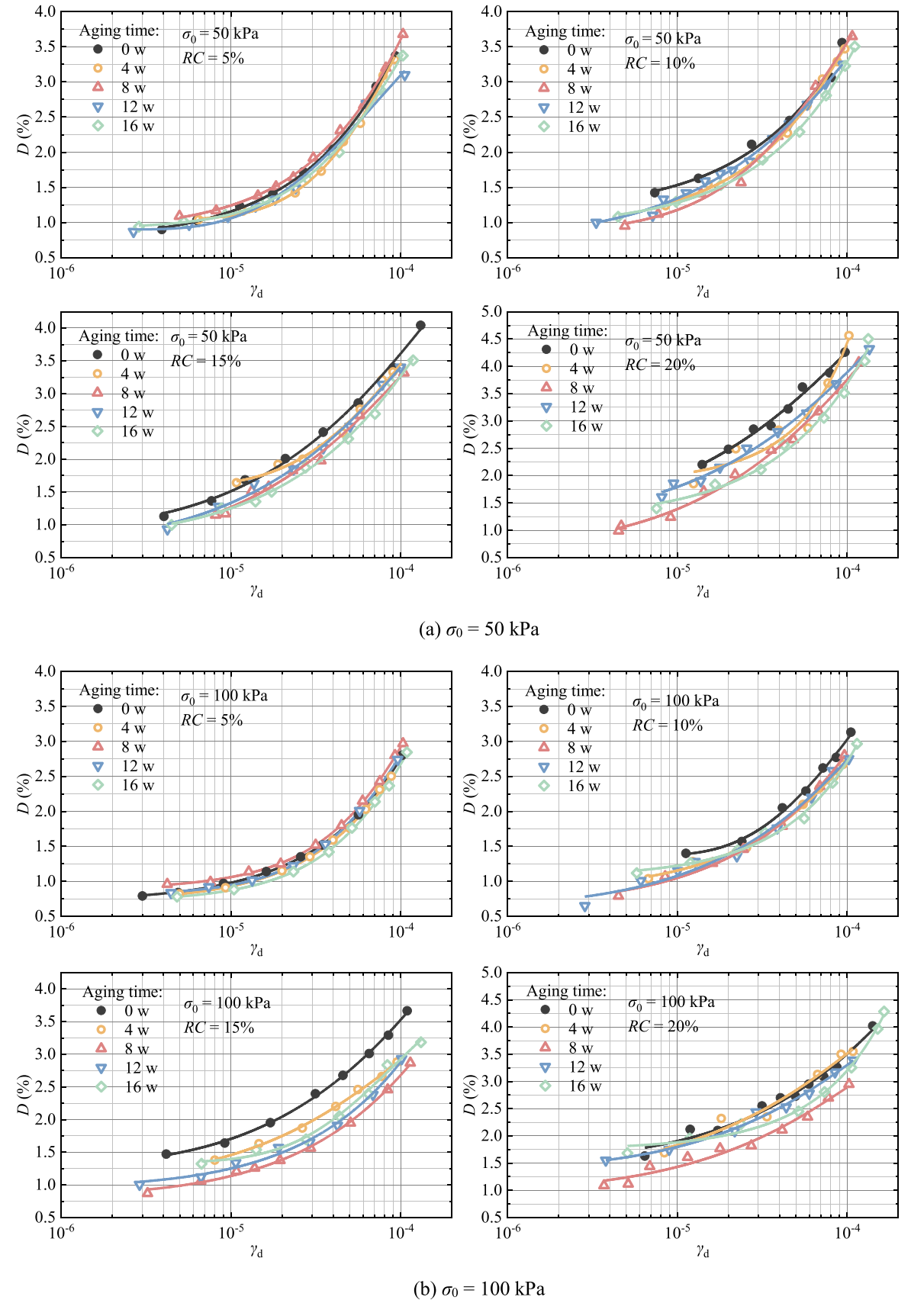


Fig. 11. The influence of rubber aging on the damping ratio of RSM.

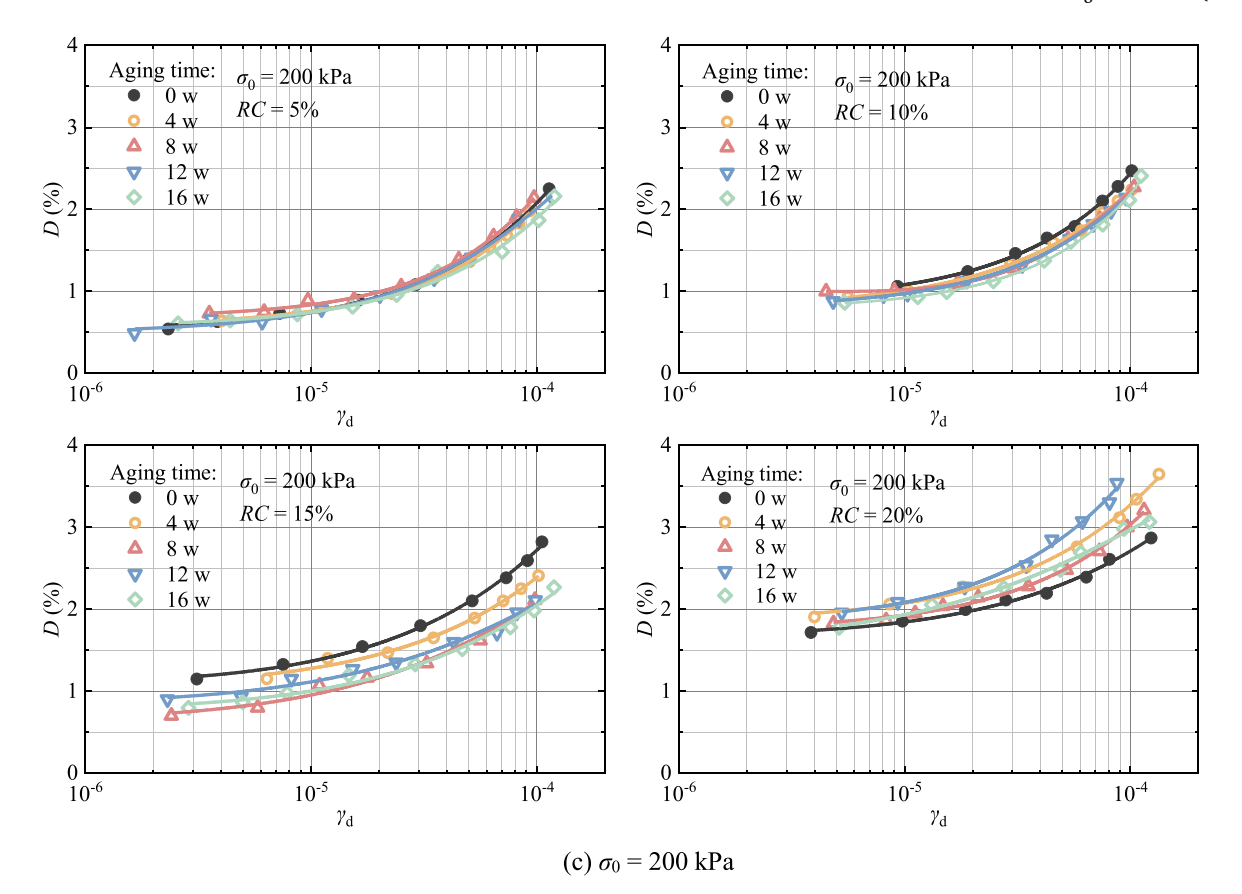


Fig. 11. (continued).

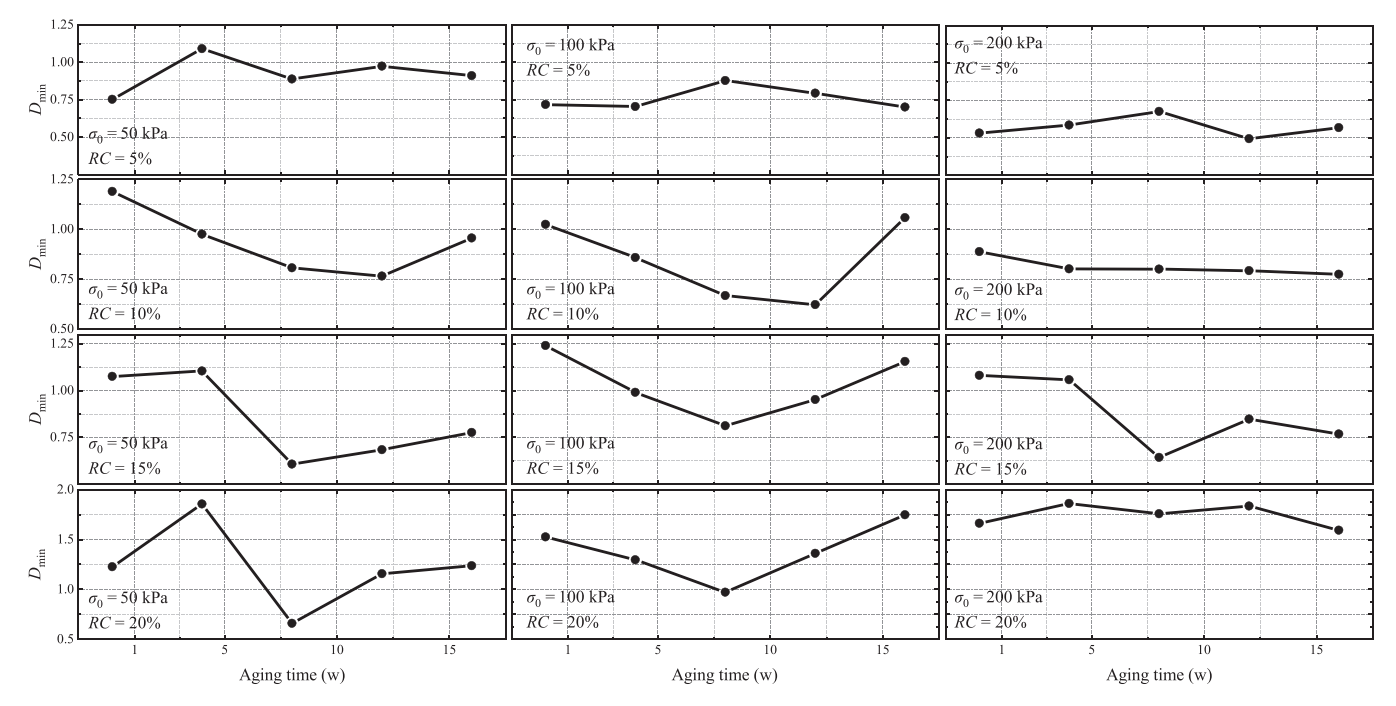


Fig. 12. The influence of rubber aging on the  $D_{\min}$  of RSM.

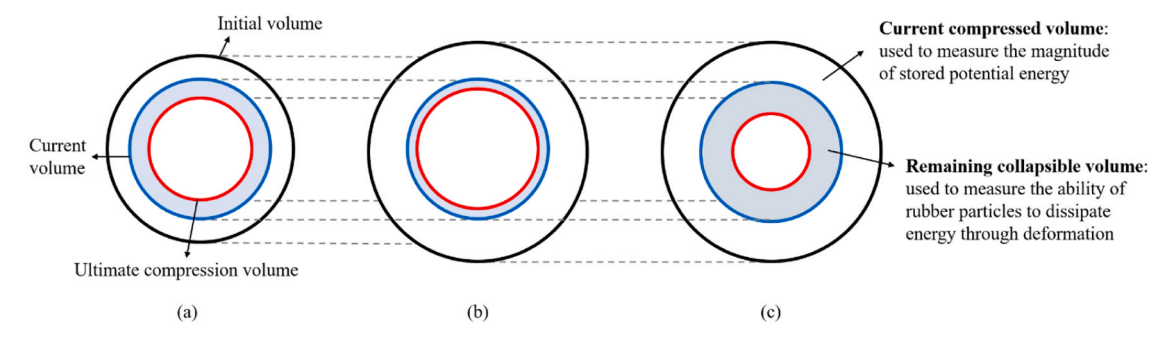


Fig. 13. Deformation diagram of rubber particles with different degrees of aging under external force.

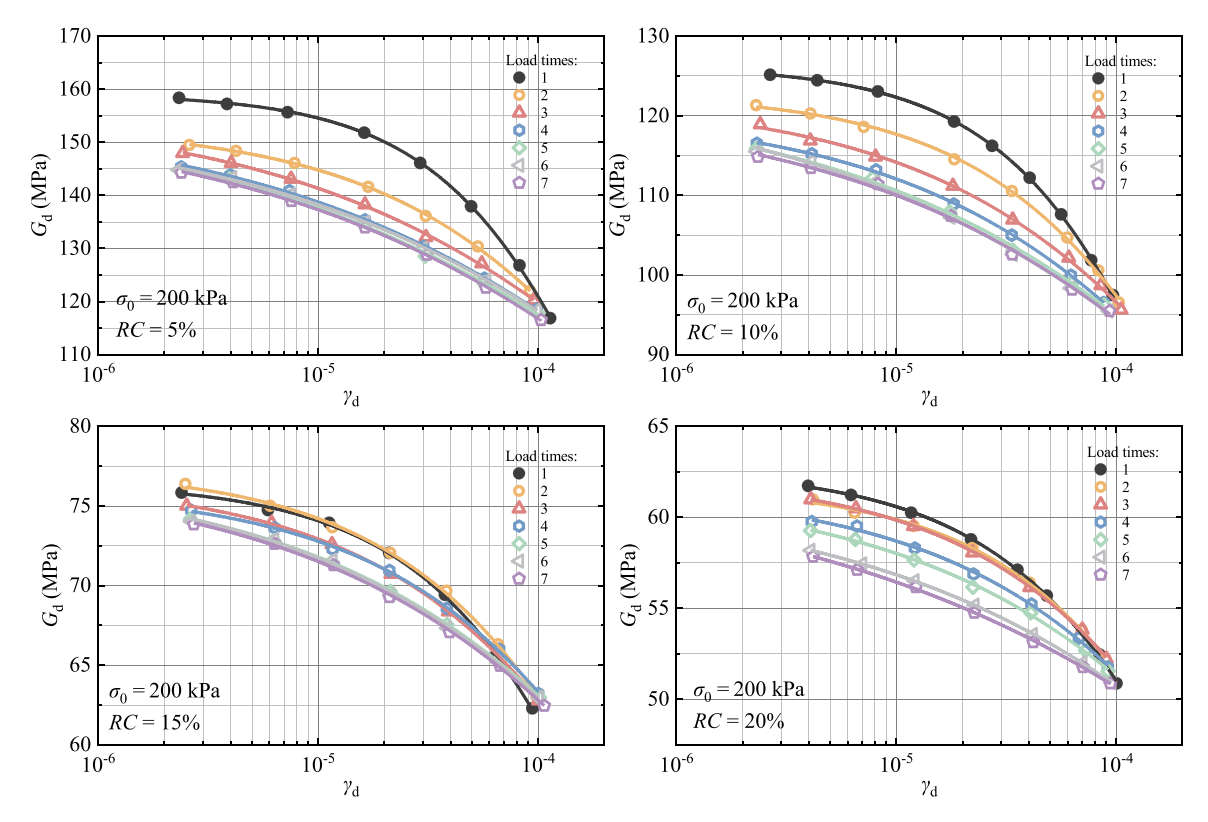


Fig. 14. The influence of loading history on the dynamic shear modulus of RSM.

$$c2 = 0.0805\alpha^2 - 0.0710\alpha + 0.0095 \tag{7}$$

$$c3 = -0.0005\alpha^2 + 0.0002\alpha + 0.0003 \tag{8}$$

where  $D_{
m masing}$  is the Masing hysteresis criterion expected damping ratio;  $D_{
m min}$  is the minimum damping ratio; b is the damping ratio curve parameters. This formula has been improved based on the H-D dynamic characteristic equation and can be widely applied to simulate the damping ratio of conventional soil. The fitting curves of the damping ratio curve under various experimental conditions are plotted as thin solid lines in Fig. 11.

The  $D_{\min}$  values for each specimen are listed in Fig. 12. As the degree of rubber aging increases, the  $D_{\min}$  of RSM first decreases and then increases, forming an inflection point between 8 and 12 weeks of aging. Moreover, the larger the RC, the more pronounced this pattern becomes. This may be because, in the early stages of rubber aging, the rubber particles in RSM expand in volume. Still, since the controlled density of the specimen remains unchanged, the degree of compression of the rubber particles within the specimen increases. The potential energy stored within the particles becomes larger. At this time, the ability of the

rubber particles to dissipate energy through deformation is weakened (Fig. 13b), leading to a decrease in the damping ratio of RSM. As the aging of rubber progresses, the elastic modulus of the rubber particles decreases, the potential energy stored within the particles is reduced, and the deformation capacity of the rubber particles increases. At this point, the ability of the rubber particles to dissipate energy through deformation is somewhat restored (Fig. 13c), and the damping ratio of RSM begins to rise. Overall, after aging treatment, the damping ratio of RSM shows a decreasing trend, which is mainly due to the degradation of the compression performance of rubber particles during the aging process.

## 3.2. Influence of loading history

## 3.2.1. Dynamic shear modulus

RSM with different proportions were tested under a confining pressure of 200 kPa. Multiple loadings were applied to each specimen, and the resulting dynamic shear modulus curves for each test are shown in Fig. 14. As the number of loadings increases, the dynamic shear modulus curves of the RSM gradually decrease, with the rate of decrease slowing

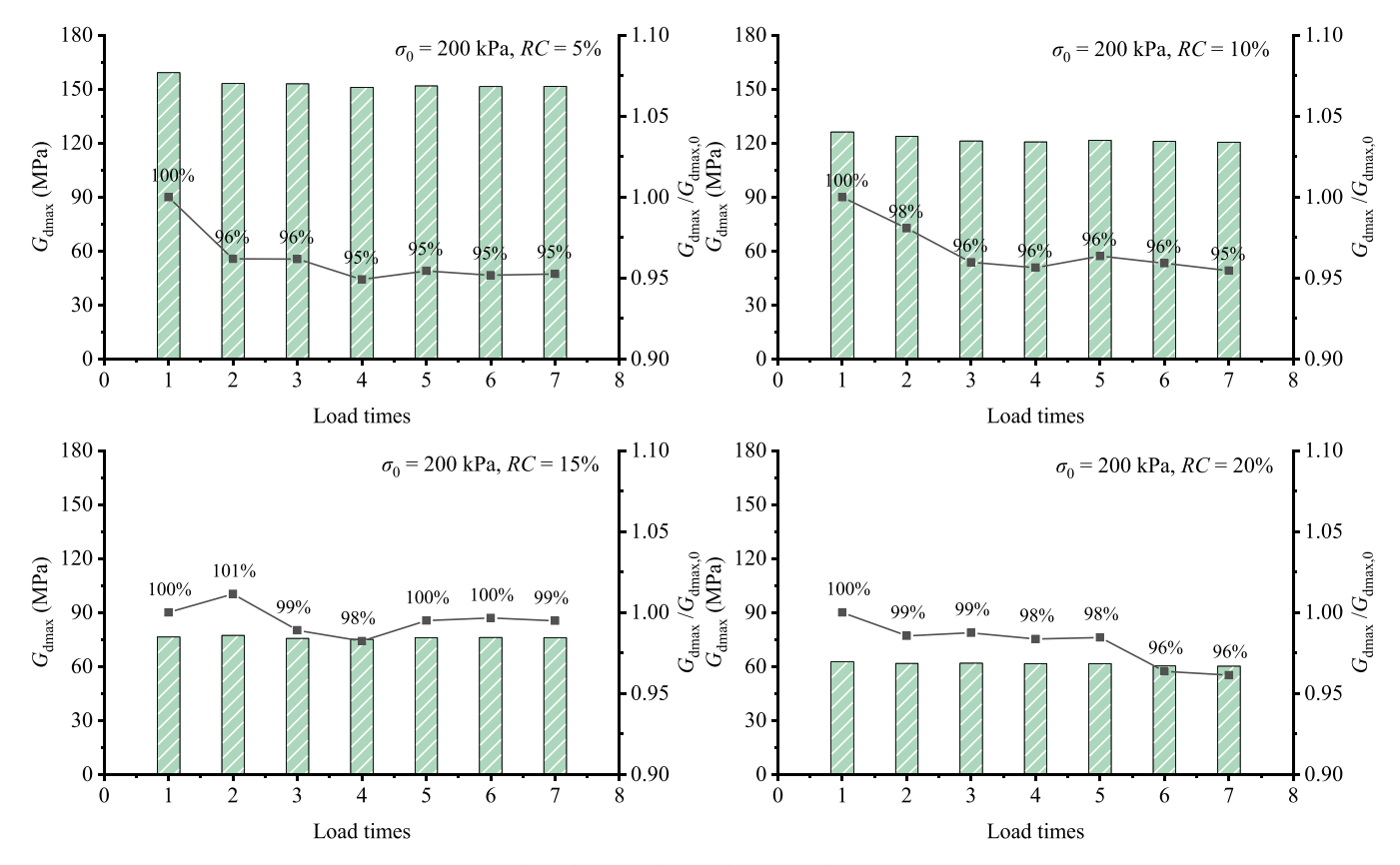


**Fig. 15.** The influence of loading history on the  $G_{\text{dmax}}$  of RSM.

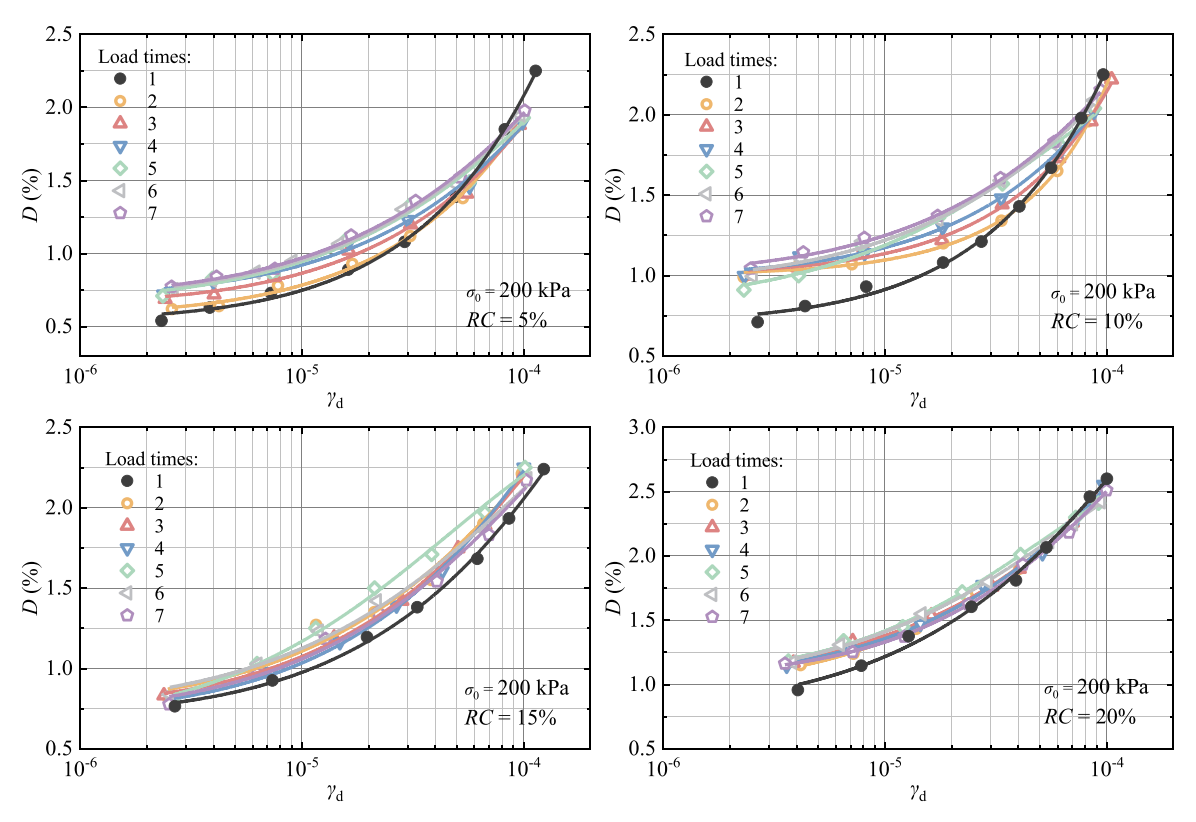


Fig. 16. The influence of loading history on the damping ratio of RSM.

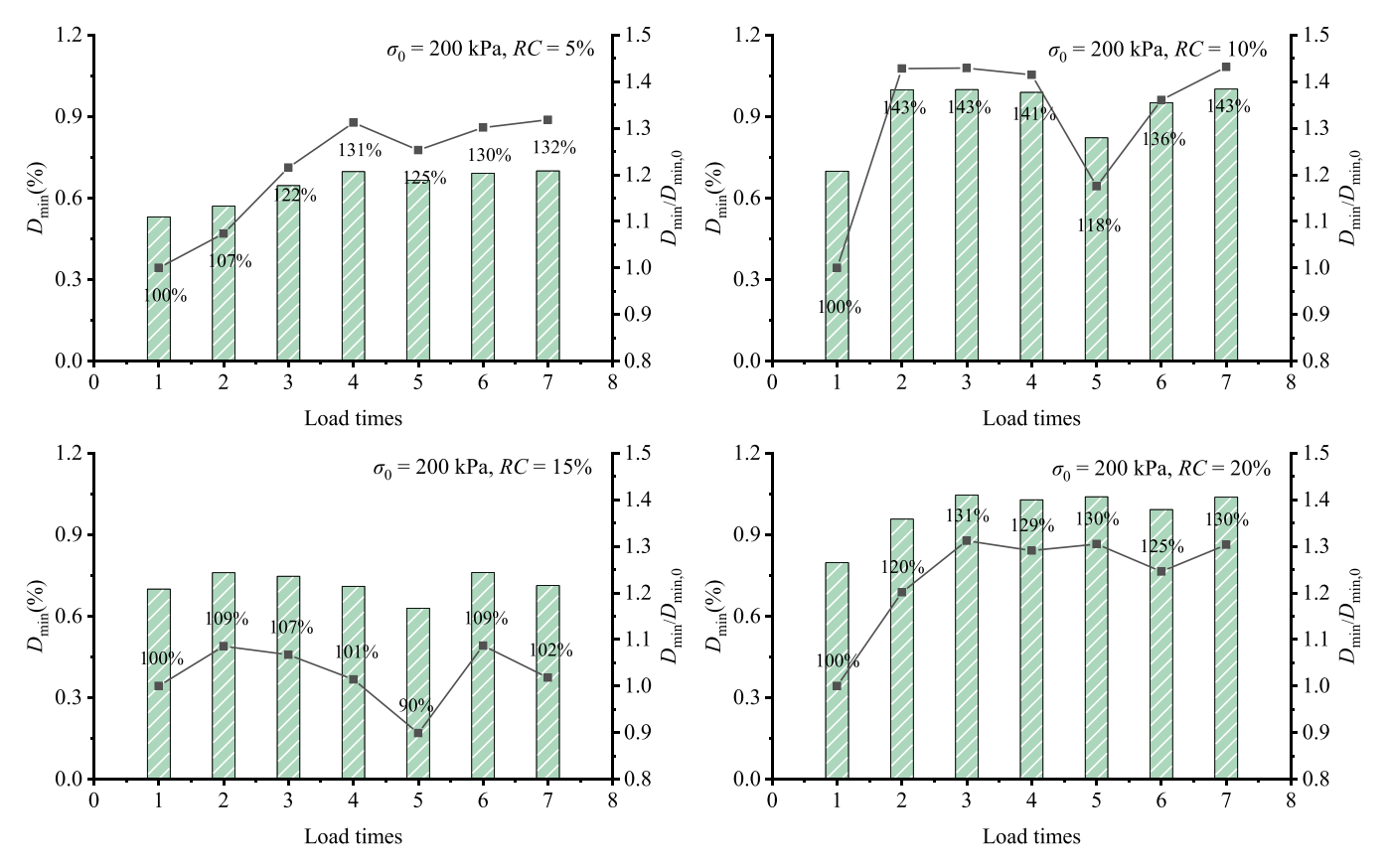
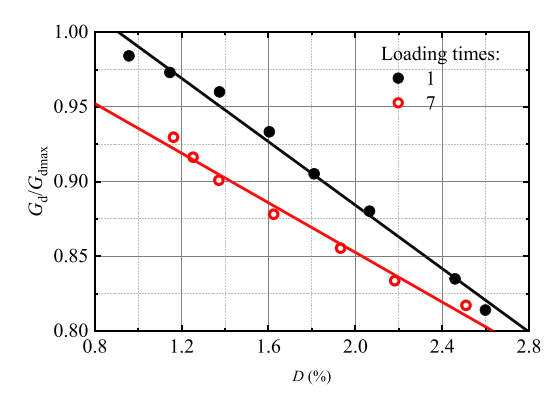


Fig. 17. The influence of loading history on the  $D_{\min}$  of RSM.



**Fig. 18.** The influence of loading history on  $G_d/G_{dmax}\sim D_d$  curves of RSM.

down and tending towards stability. The measured data were fitted using Eq. (2), and the corresponding  $G_{\rm dmax}$  values were recorded in Fig. 15. For RSM with different proportions, the  $G_{\rm dmax}$  shows a decreasing trend with the increase in the number of loadings. Zhou et al. [62] previously investigated the impact of seismic cyclic loading history on the small-strain shear modulus of saturated sand. Similar observations were made in this study: the shear modulus of the soil samples progressively decreased with the increasing number of external force disturbances. From Fig. 15, it can be observed that the decrease in  $G_{\rm dmax}$  with the increase in the number of loadings does not exceed 5 % of the initial value. Moreover, as the RC increases, the magnitude of the decrease in  $G_{\rm dmax}$  diminishes.

During the compaction process, the specimen is subjected to the impact of a compaction hammer. Subsequently, it undergoes prolonged consolidation under elevated confining pressures, resulting in a state of high density and a substantial dynamic shear modulus. In resonant

column testing, each application of force introduces disturbances to the specimen. These disturbances from external forces induce a reorganization of the tightly packed particles within the sample, leading to a reduction in density and a consequent decrease in dynamic shear modulus.

Furthermore, under the influence of confining pressure and external forces, the sand particles within the sample experience relative displacement at high pressures, which may result in the rounding of particle edges and even particle breakage. Such processes diminish the inter-particle friction, contributing to a further reduction in the dynamic shear modulus.

Rubber particles, with their inherent elasticity, can mitigate damage through elastic deformation when subjected to external forces. The presence of rubber particles also acts as a cushion, reducing the degree of edge rounding and breakage of sand particles. Consequently, an increase in the RC can attenuate the effects of loading history on the dynamic shear modulus of the RSM. This suggests that the incorporation of an appropriate proportion of rubber particles into a sand cushion layer enhances its stability when subjected to external disturbances.

#### 3.2.2. Damping ratio

The damping ratio test data for the Rubberized Sand Mixture (RSM) subjected to various loading cycles are depicted in Fig. 16. As the number of loading cycles increases, the damping ratio curve of the RSM gradually ascends. This trend correlates with the degradation of sand particles, where the rounding of particle edges facilitates easier relative displacement. Upon external energy disturbances, the sand particles can actively dissipate energy through this relative displacement, thereby enhancing the damping ratio of the specimen.

Using Eq. (3) to fit the damping ratio data of RSM, the corresponding  $D_{\min}$  is obtained, as illustrated in Fig. 17. The  $D_{\min}$  of RSM increases with the number of load cycles, showing substantial variation, with a peak increase of up to 143 % compared to the initial value (when the number

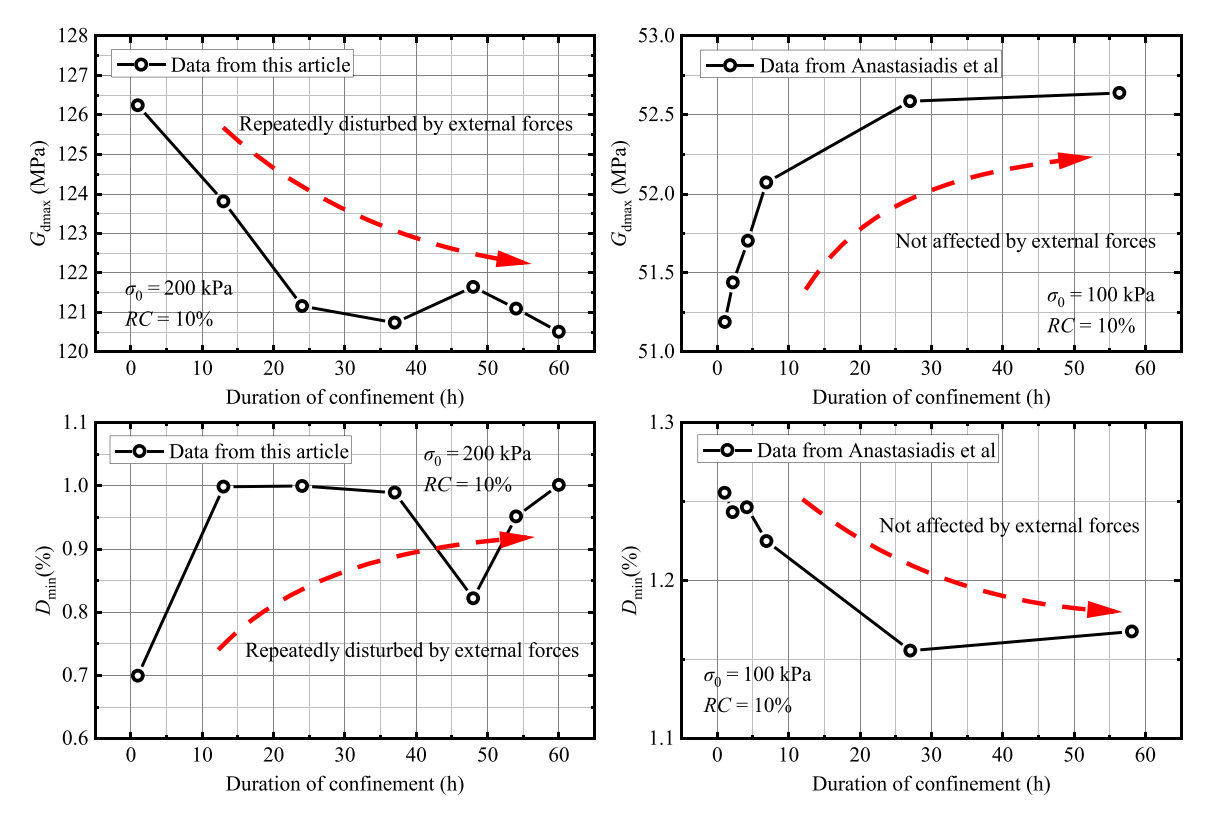


Fig. 19. Comparison of data from this article with data from Anastasiadis et al.

of load cycles is 1).

There is a linear relationship between the damping ratio of RSM and the degree of reduction in shear modulus. We plotted the  $G_{\rm d}/G_{\rm dmax}\sim D$  curves for different loading conditions, including single and multiple load cycles. As shown in Fig. 18, the linear relationship between the damping ratio and the reduction in shear modulus remains consistent across different loading histories. External loading does not disrupt this linearity; however, the slopes of the fitted lines differ, further demonstrating that the loading history affects the dynamic characteristics of RSM. Based on the different slopes, we can see that with the increase in loading times, the attenuation of the dynamic shear modulus of RSM is more significant compared to the increase of the damping ratio.

In studying the effects of loading history, it is important to note that the samples were consistently subjected to an effective confining pressure of 200 kPa. The impact of prolonged consolidation on the samples cannot be overlooked. Consolidation time is a significant factor contributing to the Time-Dependent Behavior of RSM. In the field of geotechnics, a consensus has emerged regarding the influence of consolidation time on sandy materials: as consolidation time increases, the dynamic shear modulus rises while the damping ratio decreases. Anastasiadis et al. [53] have previously studied the effects of consolidation time on the dynamic shear modulus and damping ratio of RSM, and their findings align with the conclusions mentioned earlier. As illustrated in Fig. 19, graphs a and c represent our data, where multiple resonant column tests were conducted during the consolidation process to induce disturbances in the samples. Graphs b and d correspond to the research data from Anastasiadis et al., in which the samples were not disturbed until the consolidation time reached a specified value.

It is evident that when the samples are subjected solely to confining pressure, the maximum dynamic shear modulus increases with consolidation time, while the minimum damping ratio decreases. However, applying external loading during this period results in an opposite trend. Compared to Anastasiadis et al.'s research, our samples were not only affected by the duration of confinement but also repeatedly disturbed by external forces. It is these additional disturbances that have led to our

test results showing an opposite trend to those found by Anastasiadis et al. Therefore, we can assume that the effect of loading history on RSM's dynamic characteristics is shown after the effect of consolidation time is offset. In other words, with the increase of loading times, the dynamic shear modulus of RSM decreases and the damping ratio increases, and this law still holds. This also indicates that RSM does not reduce its seismic and vibration-damping capabilities when subjected to environmental disturbances, further confirming the feasibility of using RSM as a vibration isolation layer.

## 3.3. Discussion

This study provides an analysis of how rubber aging and loading history influence the dynamic properties of RSM. The findings reveal that while the aging of rubber materials does modify the dynamic characteristics of RSM, its effect is comparatively minor relative to other factors, such as rubber content and confining pressure. Additionally, with an increasing number of loading cycles, the dynamic shear modulus of RSM exhibits a gradual decline, while the damping ratio shows a corresponding upward trend. From the perspective of vibration isolation performance, the loading history has a negligible impact on RSM. Consequently, RSM proves to be highly suitable for use in engineering environments that experience frequent vibrations, such as those surrounding railway systems. In conclusion, the influence of these factors on the operating state of RSM is limited, further reinforcing its viability as a seismic isolation layer.

With the diversity of construction environments, factors affecting Time-Dependent Behavior effects also become complex and variable. Although this paper has covered some key factors, to understand the behavior of RSM in practical applications fully, there are many other factors worthy of in-depth study. For instance, the erosion by chemical substances, the impact of microbial activity, and the potential role of groundwater are aspects that should not be overlooked in future research. These factors may significantly affect the performance and durability of RSM, and therefore, they require more in-depth discussion

and analysis in future studies.

#### 4. Conclusions

The thermal aging degree of rubber particles was enhanced using an oven method, and the compression performance of rubber particles at different aging degrees was tested. Subsequently, a series of resonant column tests were conducted to examine the effects of Time-Dependent Behavior on the dynamic characteristics of RSM, focusing primarily on two factors: the degree of rubber aging and loading history. The conclusions are summarized as follows:

- Thermal aging treatment leads to an increase in the size and expansion of rubber particles. As the degree of aging increases, their compressive performance decreases.
- (2) (The maximum dynamic shear modulus of RSM increases with increasing confining pressure and decreases with increasing *RC*. The damping ratio, on the other hand, decreases with increasing confining pressure and increases with increasing *RC*.
- (3) During the process of rubber aging, the dynamic shear modulus of RSM will fluctuate, but it generally shows a downward trend. At the same time, the damping ratio of RSM will also decrease overall due to rubber aging, with a relatively low degree of variation.
- (4) As the number of loading cycles increases, the dynamic shear modulus of RSM shows a decreasing trend, while its damping ratio gradually increases. These changes are significant and have a large magnitude.

#### CRediT authorship contribution statement

Kai Zheng: Conceptualization, Methodology, Investigation, Formal analysis, Writing – original draft. Mengtao Wu: Formal analysis, Data curation, Writing – original draft. Jun Yang: Conceptualization, Investigation, Writing – review & editing. Wei Liang: Visualization, Resources; Jie He: Conceptualization, Funding acquisition. Fangcheng Liu: Conceptualization, Funding acquisition, Resources, Investigation, Writing – review & editing.

## **Declaration of Competing Interest**

The authors declare that they have no known competing financial interests or personal relationships that could have appeared to influence the work reported in this paper.

## Acknowledgments

This research was sponsored by the Key Research Project of Hunan Provincial Department of Education under Grant No. 21A0357, the Natural Science Foundation of China under Grant No. 52308500, the Natural Science Foundation of Hunan Province under Grant No. 2021JJ40171, the Postdoctoral Fellowship Program of CPSF under Grant No. GZB20230487, and the Sichuan Science and Technology Program under Grant No. 2024NSFSC0912.

#### Data availability

Data will be made available on request.

#### References

[1] A. Mohajerani, L. Burnett, J.V. Smith, S. Markovski, G. Rodwell, M.T. Rahman, H. Kurmus, M. Mirzababaei, A. Arulrajah, S. Horpibulsuk, Recycling waste rubber tyres in construction materials and associated environmental considerations: a review, Resour. Conserv. Recycl. 155 (2020) 104679.

- [2] A.J. Bowles, A.L. Wilson, G.D. Fowler, Synergistic benefits of recovered carbon black demineralisation for tyre recycling, Resour. Conserv. Recycl. 198 (2023) 107124.
- [3] R. Raeesi, A. Soltani, R. King, M.M. Disfani, Field performance monitoring of waste tire-based permeable pavements, Transp. Geotech. 24 (2020) 100384.
- [4] H. Liu, J. Mead, R. Stacer, Environmental effects of recycled rubber in light-fill applications, Rubber Chem. Technol. 73 (3) (2000) 551–564.
- [5] H.H. Tsang, Seismic isolation by rubber–soil mixtures for developing countries, Earthq. Eng. Struct. Dyn. 37 (2) (2008) 283–303.
- [6] A. Duda, M. Kida, S. Ziembowicz, P. Koszelnik, Application of material from used car tyres in geotechnics—an environmental impact analysis, PeerJ 8 (2020) e9546.
- [7] R. Maeda, B. Finney, Water quality assessment of submerged tire-derived aggregate fills, J. Environ. Eng. 144 (2) (2018) 04017105.
- [8] K. Gabryś, Geomechanical characterization of crushed concrete-rubber waste mixtures, Sustainability 15 (19) (2023) 14446.
- [9] C.M. Arachchige, B. Indraratna, Y. Qi, C. Rujikiatkamjorn, Experimental study of rubber intermixed ballast stratum subjected to monotonic and cyclic loads, Geo-Congr. 2023 (2023) 565–574.
- [10] S.B. Reddy, A.M. Krishna, Recycled tire chips mixed with sand as lightweight backfill material in retaining wall applications: an experimental investigation, Int. J. Geosynth. Ground Eng. 1 (2015) 1–11.
- [11] A. Edinçliler, G. Baykal, A. Saygılı, Influence of different processing techniques on the mechanical properties of used tires in embankment construction, Waste Manag. 30 (6) (2010) 1073–1080.
- [12] J. Tweedie, D. Humphrey, T. Sandford, Tire shreds as lightweight retaining wall backfill: active conditions, J. Geotech. Geoenviron. Eng. 124 (11) (1998) 1061–1070.
- [13] M. Christ, J.-B. Park, S.-S. Hong, Laboratory observation of the response of a buried pipeline to freezing rubber-sand backfill, J. Mater. Civ. Eng. 22 (9) (2010) 943–950.
- [14] G. Tavakoli Mehrjardi, S. Moghaddas Tafreshi, A. Dawson, Numerical analysis on Buried pipes protected by combination of geocell reinforcement and rubber-soil mixture, Int. J. Civ. Eng. 13 (2) (2015).
- [15] S.M. Tafreshi, G.T. Mehrjardi, A. Dawson, Buried pipes in rubber-soil backfilled trenches under cyclic loading, J. Geotech. Geoenviron. Eng. 138 (11) (2012) 1346–1356.
- [16] U. Patil, J.R. Valdes, T.M. Evans, Swell mitigation with granulated tire rubber, J. Mater. Civ. Eng. 23 (5) (2011) 721–727.
- [17] H. Sotani-Jigheh, M. Asadzadeh, V. Marefat, Effects of tire chips on shrinkage and cracking characteristics of cohesive soils, Turk. J. Eng. Environ. Sci. 37 (3) (2013).
- [18] S. Yoon, M. Prezzi, N.Z. Siddiki, B. Kim, Construction of a test embankment using a sand-tire shred mixture as fill material, Waste Manag. 26 (9) (2006) 1033–1044.
- [19] Y. Ding, J. Zhang, X. Chen, X. Wang, Y. Jia, Experimental investigation on static and dynamic characteristics of granulated rubber-sand mixtures as a new railway subgrade filler, Constr. Build. Mater. 273 (2021) 121955.
- [20] M. Wu, W. Tian, J. He, F. Liu, J. Yang, Seismic isolation effect of rubber-sand mixture cushion under different site classes based on a simplified analysis model, Soil Dyn. Earthq. Eng. 166 (2023) 107738.
- [21] S. Brunet, J.C. de la Llera, E. Kausel, Non-linear modeling of seismic isolation systems made of recycled tire-rubber, Soil Dyn. Earthq. Eng. 85 (2016) 134–145.
- [22] F. Liu, D. Ren, N. Liu, C. Zhao, Numerical simulation on the isolation effect of geocell reinforced rubber-sand mixture cushion earthquake base isolator, China Civ. Eng. J. (2015).
- [23] K. Pitilakis, S. Karapetrou, K. Tsagdi, Numerical investigation of the seismic response of RC buildings on soil replaced with rubber–sand mixtures, Soil Dyn. Earthq. Eng. 79 (2015) 237–252.
- [24] H.H. Tsang, S. Lo, X. Xu, M.Neaz Sheikh, Seismic isolation for low-to-medium-rise buildings using granulated rubber-soil mixtures: numerical study, Earthq. Eng. Struct. Dvn. 41 (14) (2012) 2009–2024.
- [25] B.-B. Dai, Q. Liu, X. Mao, P.-Y. Li, Z.-Z. Liang, A reinterpretation of the mechanical behavior of rubber-sand mixtures in direct shear testing, Constr. Build. Mater. 363 (2023) 129771.
- [26] M.S. Mashiri, J.S. Vinod, M.N. Sheikh, Constitutive model for sand–tire chip mixture, Int. J. Geomech. 16 (1) (2016) 04015022.
- [27] Y. Wang, Y. Cheng, G. Yang, Y. Xie, H. Huang, R. Liu, Study on the inhibitory effect of rubber on particle breakage and the impact on the volumetric deformation of calcareous sand under different loading modes, Constr. Build. Mater. 414 (2024) 135014.
- [28] E.G. Ranjbar, E.S. Hosseininia, Seismic performance of rubber-sand mixture as a geotechnical seismic isolation system using shaking table test, Soil Dyn. Earthq. Eng. 177 (2024) 108395.
- [29] J. Wang, M. Wu, F. Liu, J. Bin, J. He, Rubber-sand infilled soilbags as seismic isolation cushions: experimental validation, Geosynth. Int. 23 (2024) 1–14.
- [30] A.K. Panah, A. Khoshay, A new seismic isolation system: sleeved-pile with soil-rubber mixture, Int. J. Civ. Eng. 13 (2) (2015) 124–132.
- [31] S. Bandyopadhyay, A. Sengupta, G. Reddy, Performance of sand and shredded rubber tire mixture as a natural base isolator for earthquake protection, Earthq. Eng. Eng. Vib. 14 (2015) 683–693.
- [32] Z. Yin, H. Sun, L. Jing, R. Dong, Geotechnical seismic isolation system based on rubber-sand mixtures for rural residence buildings: shaking table test, Materials 15 (21) (2022) 7724.
- [33] J. Bernal-Sanchez, J. McDougall, M. Miranda, D. Barreto, Dynamic behaviour of a geotechnical seismic isolation system with rubber-sand mixtures to enhance seismic protection, 3rd Eur. Conf. Earthq. Eng. Seismol., Buchar. (2022).

- [34] F. Liu, J. Wang, B. Zhou, M. Wu, J. He, J. Bin, Shaking table study on rubber-sand mixture cored composite block as low-cost isolation bearing for rural houses, J. Build. Eng. 76 (2023) 107413.
- [35] N. Madani, I. Hosseinpour, M. Payan, K. Senetakis, Cyclic and postcyclic interface characteristics of geotextile-embedded sand-rubber composites, J. Mater. Civ. Eng. 35 (2) (2023) 04022418.
- [36] M. Wu, F. Liu, J. Yang, Stress-strain-strength behavior of geosynthetic reinforced rubber-sand mixtures, Acta. Geotech. 18 (2023) 4835–4846.
- [37] J. Lopera Perez, C. Kwok, K. Senetakis, Investigation of the micro-mechanics of sand-rubber mixtures at very small strains, Geosynth. Int. 24 (1) (2017) 30–44.
- [38] J. Zhang, X. Chen, J. Zhang, P. Jitsangiam, X. Wang, DEM investigation of macroand micro-mechanical properties of rigid-grain and soft-chip mixtures, Particuology 55 (2021) 128–139.
- [39] M. Wu, F. Liu, Z. Li, G. Bu, Micromechanics of granulated rubber-soil mixtures as a cost-effective substitute for geotechnical fillings, Mech. Adv. Mater. Struct. 30 (13) (2023) 2701–2717.
- [40] M. Payan, K. Senetakis, Effect of anisotropic stress state on elastic shear stiffness of sand-silt mixture, Geotech. Geol. Eng. 37 (3) (2019) 2237–2244.
- [41] A. Shafiee, A. Hassanipour, M. Payan, S. Bahmani Tajani, R. Jamshidi Chenari, Analysis of the stiffness and damping characteristics of compacted sand-in-fines granular composites: a multiscale investigation, Granul. Matter 24 (3) (2022) 87.
- [42] N. Khodkari, P. Hamidian, H. Khodkari, M. Payan, A. Behnood, Predicting the small strain shear modulus of sands and sand-fines binary mixtures using machine learning algorithms, Transp. Geotech. 44 (2024) 101172.
- [43] M. Zamanian, V. Mollaei-Alamouti, M. Payan, Directional strength and stiffness characteristics of inherently anisotropic sand: the influence of deposition inclination, Soil Dyn. Earthq. Eng. 137 (2020) 106304.
- [44] K. Senetakis, A. Anastasiadis, K. Pitilakis, Dynamic properties of dry sand/rubber (SRM) and gravel/rubber (GRM) mixtures in a wide range of shearing strain amplitudes, Soil Dyn. Earthq. Eng. 33 (1) (2012) 38–53.
- [45] G. Banzibaganye, C. Vrettos, Resonant column tests on mixtures of different sands with coarse tyre rubber chips, Geotech. Geol. Eng. 40 (12) (2022) 5725–5738.
- [46] F. Liu, K. Zheng, B. Jia, J. Yang, M. Wu, Shear modulus and damping ratio of granulated rubber-sand mixtures: influence of relative particle size, Constr. Build. Mater. 427 (2024) 136205.
- [47] B. Madhusudhan, A. Boominathan, S. Banerjee, Cyclic simple shear response of sand–rubber tire chip mixtures, Int. J. Geomech. 20 (9) (2020) 04020136.
- [48] E.T. Bowman, K. Soga, Mechanisms of setup of displacement piles in sand: laboratory creep tests, Can. Geotech. J. 42 (5) (2005) 1391–1407.

- [49] G. Li, C. Guo, X. Gao, Y. Ji, O. Geng, Time dependence of carbonation resistance of concrete with organic film coatings, Constr. Build. Mater. 114 (2016) 269–275.
- [50] Y.-R. Zhang, Y. Zhang, J. Huang, H.-X. Zhuang, J.-Z. Zhang, Time dependence and similarity analysis of peak value of chloride concentration of concrete under the simulated chloride environment, Constr. Build. Mater. 181 (2018) 609–617.
- [51] S. Wang, Y. Li, R. Yang, B. Xu, B. Lu, Rheological behavior with time dependence and fresh slurry liquidity of cemented aeolian sand backfill based on response surface method, Constr. Build. Mater. 371 (2023) 130768.
- [52] J. Guo, X. Chen, Pressure dependence of elastic wave velocities of unconsolidated cemented sands, Geophysics 87 (4) (2022) MR161–MR175.
- [53] A. Anastasiadis, K. Senetakis, K. Pitilakis, C. Gargala, I. Karakasi, Dynamic behavior of sand/rubber mixtures. Part I: effect of rubber content and duration of confinement on small-strain shear modulus and damping ratio, J. ASTM Int. 9 (2) (2012) 1–19.
- [54] D.R. Bauer, J.M. Baldwin, K.R. Ellwood, Rubber aging in tires. Part 2: accelerated oven aging tests, Polym. Degrad. Stab. 92 (1) (2007) 110–117.
- [55] N. Rodriguez, L. Dorogin, K. Chew, B. Persson, Adhesion, friction and viscoelastic properties for non-aged and aged Styrene Butadiene rubber, Tribology Int. 121 (2018) 78–83.
- [56] M. Safari, M. Rowshanzamir, S.M. Hejazi, M. Banitalebi-Dehkordi, Combined effect of end-of-life rubber and a hydrophobic polymer on coastal saturated sand: a multiaspect investigation, J. Mater. Civ. Eng. 35 (3) (2023) 04022439.
- [57] A.Y. Akhtar, H.-H. Tsang, Dynamic properties of recycled polyurethane-coated rubber-soil mixtures, Case Stud. Constr. Mater. 18 (2023) e01859.
- [58] L. Liu, G. Cai, S. Liu, Corrigendum to "Compression properties and micromechanisms of rubber-sand particle mixtures considering grain breakage" [J. Constr. Build. Mater. 187 (2018) 1061–1072], Constr. Build. Mater. 195 (2018), 695-695
- [59] A. ASTM, D4015–15: Standard Test Methods for Modulus and Damping of Soils by Fixed-base Resonant Column Devices, ASTM International, West Conshohocken, 2015
- [60] B.O. Hardin, V.P. Drnevich, Shear modulus and damping in soils: design equations and curves, J. Soil Mech. Found. Div. 98 (7) (1972) 667–692.
- [61] M.B. Darendeli, Dynamic properties of soils subjected to 1994 Northridge earthquake, University of Texas at Austin, 1997.
- [62] Y.G. Zhou, Y.M. Chen, Influence of seismic cyclic loading history on small strain shear modulus of saturated sands, Soil Dyn. Earthq. Eng. 25 (5) (2005) 341–353.